QUANTIFICATION OF ICING LOSSES IN WIND FARMS

REPORT 2016:299

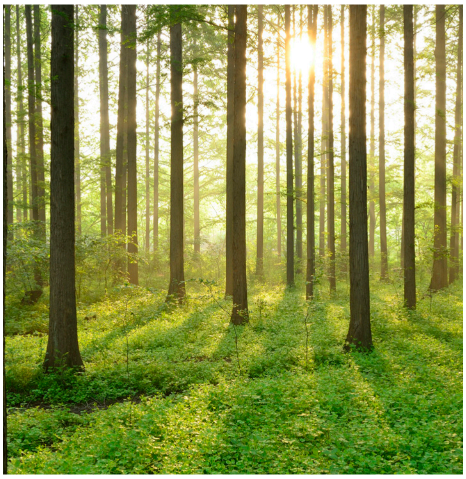

VINDFORSK

Energiforsk

Quantification of icing losses in wind farms

Assessment and optimization of the energy production of operational wind farms: Part 3

JOHAN HANSSON, JOHANNES LINDVALL, ØYVIND BYRKJEDAL
KJELLER VINDTEKNIKK
SPRING 2016

ISBN 978-91-7673-299-1 |

Energiforsk AB | Phone: 08-677 25 30 | E-mail: kontakt@energiforsk.se | www.energiforsk.se

Foreword

Icing of wind turbine blades poses a great challenge for wind farms in cold climate. Some wind farms can suffer production losses of more than 10 % of the annual energy production. Knowledge of how the production is affected by icing is of great importance, especially since a large part of the planned wind farms in Sweden are located in the north. Post-construction production assessment, that is, estimating production and losses in operating wind farms, provide valuable insights in this question.

The aim of the project "Assessment and optimization of the energy production of operational wind farms" is to develop methods for post-construction production assessment, and to identify ways to optimize wind power production in operating wind farms. The project has been divided in three parts: Part 1 - Post-construction production assessment, Part 2 - Use of remote sensing for performance optimization, and Part 3 – Quantification of icing losses. This report presents the results from Part 3.

Methods for estimating production losses in operating wind farms developed in Part 1 have been compared to existing models for estimating icing losses. The results can be used for optimizing the operation of existing wind farms, as well as facilitate the planning of new wind parks in cold climate.

This project has been carried out by Kjeller Vindteknikk, with Sónia Liléo (May 2014-June 2015) and Johan Hansson (from June 2015) as project leaders. Reference group has consisted of Johannes Derneryd (Stena Renewables) and Jenny Longworth (Vattenfall). The project has been a part of Energiforsks' research program Vindforsk IV.

Stockholm, July 2016

Åsa Elmqvist
Progam manager, Vindforsk IV

Acknowledgments by the authors

The authors would like to thank the Vindforsk – IV research program for co-funding this project, and the members of the reference group, Johannes Derneryd and Jenny Longworth, for valuable comments on the work. Many thanks also to Åsa Elmqvist at Energiforsk and Angelica Ruth at Energimyndigheten for smooth administration when the project manager was changed half way through the project. The authors also thank Stena Renewable and Vattenfall for providing wind farm data and the turbine service technicians for help with the installation of the Wind Iris lidar, and Guillaume Coubard-Mille and Marc Brodier at Avent for help and guidance during the installations of the Wind Iris and when analyzing the data measured by the Wind Iris.

Furthermore, the authors are thankful to the colleagues at Kjeller Vindteknikk for valuable discussions.

Finally, the authors would like to thank Sónia Liléo for initiating the project and for managing it until June 2015.

Sammanfattning

Detta är den tredje rapporten i projektet "Assessment and optimization of the energy production of operational wind farms". Undertiteln på rapporten är "Part 3: Quantification of icing losses".

Del 3 har fokus på förluster relaterade till nedisning av vindturbiner. En stor andel av de svenska vindkraftparkerna är byggda på platser som årligen berörs av is. Produktionsförluster på grund av nedisning kan på årlig basis uppgå till mer än 10 % för de mest utsatta vindparkerna; det är av yttersta vikt att ta hänsyn till detta i produktionsuppskattningar inför byggnation. Issituationen i tre svenska vindparker studeras i projektet genom analys av observationer av produktion och vind tillsammans med information om driftstatus hos varje individuell turbin.

Att identifiera när bladen på vindkraftverken är täckta med is är den första utmaningen. I det här projektet används en tröskeleffektkurva i kombination med information om turbinens status och lufttemperaturen.

Förlustuppskattningar med hjälp av metoder som utvecklats i den första rapporten i projektet (Lindvall, Hansson, & Undheim, 2016) jämförs med modellerade förluster. Valet av metod är viktigt när det handlar om att uppskatta förluster på grund av is. Metoder som är beroende av att en eller flera turbiner i parken är fria från is, fungerar i allmänhet inte. Istället rekommenderas metoder baserade på vind, uppmätt eller modellerad, och uppmätt produktion. De modellerade förlusterna är baserade på en numerisk väderprognosmodell som använts i kombination med en modell för istillväxt. De observerade och modellerade förlusterna har god överensstämmelse.

En viktig sak att ta hänsyn till när observerade och modellerade förluster jämförs är hur turbinerna styrs då is finns på bladen. Stora skillnader mellan observationer och modellresultat kan förekomma om inte hänsyn till turbinregleringen tas i modellen. Resultaten visar att isregleringsstrategier som inte är optimala kan orsaka onödigt stora förluster.

Användning av nacellemonterad lidar väntas inte innebära några förbättringar när det gäller detektering av is på bladen eller i uppskattningen av förluster på grund av is.

Operationella energiprognoser som tar hänsyn till is har validerats för de två vindparker som har högst isfrekvens. En jämförelse mellan prognoser som inte tar hänsyn till is och prognoser som tar hänsyn till is visar på en signifikant kvalitetsförbättring för den senare.

En jämförelse mellan en nacellemonterad lidar och en nacellemonterad anemometer under perioder med och utan nedisning har gjorts. Installationen av lidarn har gjorts enligt gällande rekommendationer. Trots detta så finns det tecken som tyder på att anemometern påverkas något av lidarn. Jämförelsen är gjord på ett begränsat datamaterial och att osäkerheterna är stora. Fler mätkampanjer behövs för att bättre slutsatser skall kunna dras.

.

Summary

This is the third report of the project "Assessment and optimization of the energy production of operational wind farms". The subtitle is "Part 3: Quantification of icing losses".

Part 3 treats the issue of icing loss estimates. A large number of the Swedish wind farms are built in cold climate sites which experience atmospheric icing. The production losses caused by icing are an essential part of the pre-construction production assessment, since icing losses can be larger than 10 % of the annual energy production for the most exposed sites. Production and wind measurement data along with information of the operative status from individual turbines (WTGs) of three Swedish wind farms (WFs) in operation are analyzed in order to study the icing situation in the WFs.

To detect ice on the blades is the first challenge. A threshold power curve in combination with turbine status and temperature criteria are used in this project. This method has been found to be performing well in the literature.

Methods for estimating losses of operational wind farms developed in the Part 1 report (Lindvall, Hansson, & Undheim, 2016) are compared with modelled icing losses. It is important to select an appropriate method when icing losses are estimated. Some methods rely on neighboring turbines, which most likely also are influenced by icing. Methods based on wind speed, measured or modelled, and measured power are appropriate for periods with icing. The modelled losses are based on a numerical weather prediction (NWP) model that is used in combination with an ice accretion model. It is seen that the operational losses and modelled losses in general are in good agreement.

One important thing worth noting is that when icing losses are assessed in operational data and compared to model results, it is important to consider how the turbines are operated during periods with ice on the blades. There can be large discrepancies if the model results are not assuming the actual regulation strategy of the turbine. It is seen in the project that non-optimal regulating strategies can cause unnecessary large losses.

The use of a nacelle mounted lidar is not expected to improve the detection of ice on the turbine or the estimation of losses due to icing.

Operational short-term energy forecasts that accounts for icing are validated for the two wind farms that experience the largest amounts of icing. The forecast performance is significantly improved when icing is accounted for.

A comparison between a nacelle mounted lidar and the nacelle anemometer during icing and non-icing period is made. The mounting procedure of the lidar used in this project seems to cause a small disturbance in the measurements made by the nacelle anemometer. The result from the comparison is based on a limited data material and the uncertainties are large. More measurement campaigns are necessary in order to further study this topic.

List of content

1 Introduction

The need of accurate production estimates requires assessment methodologies that describe in a proper way the wind conditions and the wind farm performance at sites of diversified characteristics, with the most challenging ones being mountainous, forested and cold climate sites. Several national and international research and development projects have therefore been conducted during the last years aiming to develop tools and models to assess the energy production at such sites. The majority of these projects have however focused on the development of pre-construction assessment methodologies, that is, methodologies that are used to estimate the expected production of wind farms during the development phase of the wind farms.

There has been a rapid increase in the installed wind power capacity in Sweden during the last decade. Many of the projects have been developed by small companies with little or no experience from the energy business. While traditional power plants have been closely monitored and performance optimized, wind turbines have more or less been left alone. They have of course been monitored in order to avoid longer stand stills and the manufacturers require regular maintenance. Apart from perhaps one or two exceptions, detailed analyses of production data in order to optimize the performance or to re-evaluate the long-term production have not been made.

The existence of a large number of wind farms that have been in operation during several years gives however a new perspective to the development of assessment methodologies. Operational data from existing wind farms contain valuable information on the wind conditions, and on the performance of the turbines, under the site-specific conditions. The analysis of operational data is therefore a key tool for the identification of shortcomings on the existing pre-construction assessment methodologies, and for the further development of more accurate methods.

Two other important applications of the analysis of production data from operational wind farms are the following: re-calculation of the wind farms expected energy production, so-called "post-construction assessment"; and the identification of potential optimization needs.

The project "Assessment and optimization of the energy production of operational wind farms" consists of three work packages (WPs). The first work package is called "Post-construction production assessment". Methods for long term adjustment of operational wind farm data are developed in WP1. The uncertainty in AEP estimations based on operational data is significantly reduced compared to AEP estimations based on pre-construction wind measurements. Methods used to assess losses in the operational data are also developed in WP1. The second work package is called "Use of remote sensing for performance optimization". In WP2 the use of a nacelle mounted lidar (Wind Iris) for turbine performance optimization is evaluated. The yaw alignment, the power curve, and the nacelle transfer functions are studied during four measurement campaigns in two different wind farms. This report contains the results from work package three (WP3).

WP3 treats the issue of icing loss estimation. A large number of the Swedish wind farms are built in cold climate sites which experience atmospheric icing. The production losses caused by icing are an essential part of the production assessment, since icing losses can be larger than 10 % of the annual energy production for the most exposed sites.

The objectives of WP3 are:

1. Present a description of methodologies used to estimate the icing losses of operational wind farms.
2. Present further developed tools to perform post-construction estimates of icing losses.
3. Provide results from the comparison of the icing losses estimated based on operational data with the icing losses modeled using the IceLoss model.
4. Report on the importance of the use of nacelle-mounted lidar measurements for the accuracy of the estimated icing losses.
5. Present results of the further development of the IceLoss model (Chapter 4) that leads to higher accuracy in the modeled icing losses.

2 Input data

2.1 WIND FARMS USED IN THE PROJECT

Supervisory control and data acquisition (SCADA) data from three operational onshore wind farms have been used in WP3. They are, due to confidentiality aspects, only described in general terms.

The first 6 months of operational SCADA data has been excluded from the analysis to avoid the startup phase of the wind farms to contribute with uncertainty.

2.1.1 SCADA parameters

The SCADA parameters used in the WP3 analysis are mainly the time stamp, average power, nacelle-anemometer (ultrasonic anemometers for all three wind farms) based upstream wind speed and alarm/operating state information. In addition RPM, yaw angle and temperature are used in some of the studies.

The SCADA data is provided for each wind turbine and with a 10-minute temporal resolution. Also wind direction[1] and ambient air temperature are available in the provided SCADA data. However, in terms of wind direction there was a substantial difference in the offset of the individual turbines nacelle positions and the offsets are in addition changing throughout the analyzed period. Wind direction from a long-term reference dataset (Section 2.2) is therefore used as the source for wind direction. The use of wind direction from a long-term reference dataset will introduce some additional uncertainty in the results compared to if correct on-site measurements would have been available.

Air temperature data is also taken from the reference dataset, since we have no knowledge of the location of the temperature sensor; the heat from the nacelle can create a bias.

In the provided SCADA data of the three wind farms, the level of detail regarding alarms/operating state varies substantially. The level of detail of alarm information of wind farm 1 (WF1) and wind farm 3 (WF3) enables a relatively precise filtering while less detail are provided for wind farm 2 (WF2), which results in a somewhat more conservative filtering. No external ice-detection equipment is available for any of the WFs in this analysis.

2.1.2 Wind farm 1

WF1 is located in a forested area with complex terrain experiencing rather long and harsh winters. The turbine layout consists of five 2.0 MW turbines with hub height 80 m and 12 2.0 MW turbines with hub height 105 m. The wind farm was built in two stages and only the complete park, 17 turbines, is considered in this report. The minimum distance between neighboring turbines varies from 3.5 to 10.8 rotor diameters with an average of 5.2 rotor diameters.

---

[1] The turbine types are different in the two WFs and the SCADA parameters differ slightly. From two of the wind farms the directional data is from the turbine wind vane, from the other it is from the yaw system.

SCADA data for the period 2008-08-07 to 2015-01-07 was provided by the wind farm owner. In the analysis SCADA data for the period 2009-03-01 to 2014-12-31 are used. A revision of the nacelle transfer functions (NTFs), relating the wind speed measured behind the rotor to the undisturbed wind speed up-wind of the rotor, was made during spring 2010. In terms of power curves, May 1, 2010 is therefore treated as a revision date.

2.1.3 Wind farm 2

WF2 is located in southern Sweden where the winters in general are short and mild. The terrain is rather simple and covered with production forest of varying height. WF2 is composed of 11 2.5 MW turbines with a hub height of 98.5 m. It has been operational since 2012. The minimum distance between neighboring turbines varies from 3.9 to 4.7 rotor diameters with an average of 4.1 rotor diameters.

SCADA data for the period 2012-01-01 to 2014-12-31 was provided by the wind farm owner. Considering that a major upgrade to most of the WTGs' power curve occurred in the beginning of the summer 2014 and that it is preferable to utilize full year of data to avoid seasonal bias, only data for the period 2012-06-01 to 2014-05-31 is considered in the analysis. In addition, the wind farm owner has provided us with information that the turbine manufacturer performed some changes to the operation in April 2013. In terms of power curves, April 1, 2013 is therefore treated as a revision date.

2.1.4 Wind farm 3

Wind farm 3 (WF3) is located in a forested area in northern Sweden with long and harsh winters. The terrain is considered to be complex. Icing is significant. The turbine layout consists of 40 1.8-2.0 MW turbines with hub height 95 m. SCADA data for the period 2010-12-01 – 2014-03-18 is used in the analysis. The minimum distance between neighboring turbines varies from 3.6 to 6.0 rotor diameters with an average of 4.4 rotor diameters.

2.1.5 Filtering – identifying full-performance

It is essential that erroneous data is removed from the data set so that the results are not affected. If data is removed only for specific wind situations (high/low) any statistics derived from the data set will not represent the true values for the period. Alarms related to high/low wind speeds can have this effect. Icing might also cause such effects depending on during which weather situations that icing occur. This will be site dependent. Some methods outlined in this report will not be suitable for data sets with large (seasonal) gaps. Periods when the turbines are not in full performance need to be filtered out before the data is used to evaluate the occurrence of icing.

Production is considered as partial- or non-performing when any of the following apply:

- Periods of curtailment, below the rated power.
- Periods identified as influenced by icing.
- An alarm code is found. No detailed information on the meaning of the error codes of WF2 was available. Through an analysis, an interval of operating states were identified to clearly be associated with full-performance, the remaining operating states were treated as partial- or non-performing and filtered out. The filtering of

WF2 is considered to be somewhat conservative. The time step after an alarm is also filtered out.

- Periods when neither of the above applies and the nacelle wind speed is well above cut-in wind speed but production is negligible.

2.2 LONG-TERM REFERENCE DATASETS

Since wind speed and wind direction vary from year to year, the yearly energy production will also show considerable variation from a year to another. To get an expected energy production of the wind farm averaged over its lifetime, it is necessary to long-term correct the production data. There are many methodologies to carry out this long-term correction; but common for all methods is the need of a long-term reference dataset.

The long-term time-series utilized in the present analysis origin from the dataset denoted as KVT Meso. The KVT Meso dataset is produced by Kjeller Vindteknikk using the Weather Research and Forecast model (WRF, Skamarock, et al., 2008), which is a mesoscale meteorological model used for both research and weather forecasting. The KVT Meso dataset uses FNL data (Final Global Data Assimilation System) available from the National Centers for Environmental Prediction (NCEP) as initialization and boundary data for the model. Table 2.1 summarizes the main properties of the KVT Meso dataset. More information is presented in Chapter 4.

Table 2.1. Properties of the long-term dataset KVT Meso produced by Kjeller Vindteknikk.

Long-term dataset	Horizontal resolution	Temporal resolution	Temporal coverage
KVT Meso	4 km x 4 km	1 hour	2000 – ongoing

Long-term time series of hourly wind speed, wind direction, temperature and air density are available in the KVT Meso dataset.

Several of the methods used to assess losses in the historical data (Lindvall, Hansson, & Undheim, 2016) utilize the raw SCADA data with 10 minute resolution. To avoid discarding 5/6 of the SCADA data, the hourly KVT Meso dataset (wind speed and wind direction) is linearly interpolated to 10 minute values.

3 Description of methodologies for estimation of icing losses in operational wind farms

3.1 IDENTIFICATION OF ICING PERIODS IN OPERATIONAL DATA

The first challenge, before it is possible to assess the losses, is to properly identify the periods when icing has influenced the energy production. Methods to calculate icing losses based on production data from other wind turbines of the same farm have to deal with the challenge of icing often occurring on all the turbines simultaneously. Trying to estimate the icing losses based on a comparison between summer and winter power curves is often an easy choice. However, turbulence, atmospheric stability, and air density may be substantially different during winter as compared to summer, which makes the power curve estimated based on summer data unable to represent the expected power during winter.

Other methods assume that the variations around the power curve will equal out if averaged over a sufficient long period of time, and that possible deviations from this are caused by icing. This method can give reasonable estimates of icing on long-term basis, but fails when estimating the icing losses occurred during short time periods.

Some methods use a threshold value on the power curve, and identify periods when the power production comes below this threshold value as periods with icing. However, since the power will fluctuate around a given power curve depending also on other parameters such as wind direction, atmospheric stability and turbulence, this methodology might not find all the cases when icing on the blades resulted on icing losses, and might, on the other hand, identify periods as being associated to icing losses although icing has not been a problem. In (Davis, Byrkjedal, Hahmann, Clausen, & Žagar, 2015) three methods for ice detection is described and evaluated. The method assessed to be best suited by (Davis, Byrkjedal, Hahmann, Clausen, & Žagar, 2015), a threshold power curve, is used in this report with only minor modifications. It is further described in Chapter 5.

There are different ways to estimate the losses that have occurred in an operational wind farm based on production data. Six methods are described in (Lindvall, Hansson, & Undheim, 2016), not all are suitable for estimating icing losses. Read more about this in Chapter 5.

3.2 DESCRIPTION OF METHODOLOGIES FOR ESTIMATION OF LONG-TERM ICING LOSSES OF OPERATIONAL WIND FARMS

Long term icing losses are estimated with icing climatologies. The icing climatologies are representative for the expected lifetime of the wind farm. The icing losses derived from operational data are normally not representative for long-term conditions. However, they can be used to adjust the long-term conditions from pre-construction tools. This is done in Chapter 5.

A brief overview of icing climatologies is found in Section 3.2.1. Additional information can be found in (Cattin, 2012), which is a survey of existing research in the field of icing on wind turbines and also includes an introduction to atmospheric icing.

3.2.1 Icing climatologies

Icing climatologies can be more or less advanced depending on how they are derived. The best and most sophisticated icing climatologies are based on high quality on-site measurements of relevant variables made over long periods of time. One of the relevant variables is direct measurements of ice load. Such measurements are extremely rare. Advanced alternative methods consist of using Numerical Weather Prediction (NWP) models and ice accretion models while "simpler" ones are based on publicly available weather data from airports, national meteorological stations or on-site met mast measurements of wind, temperature and humidity.

In (IEA, 2012) a methodology for site classification is presented. The method consists of investigating the frequency of

- Meteorological icing: Period during which the meteorological conditions for ice accretion are favorable (active ice formation)
- Instrumental icing: Period during which the ice remains at a structure and/or an instrument

Based on the yearly frequency of occurrence of the two parameters, a rough estimate of the annual production loss can be made.

A similar approach is proposed in (Beckford, Lindahl, & Ribeiro, 2015). The frequency of occurrence of ice on cup anemometers, ultrasonic anemometers and wind vanes have been analyzed for more than 60 met masts throughout Norway, Sweden and Finland. It is concluded that, for Sweden, there exist a linear relationship between the sensor elevation and the number of days with anemometer icing. The relationship was less clear in Norway and Finland. In combination with results from analyzing data from 18 operational wind farms in Sweden, a clear, but non-linear, relationship between the loss due to icing and the sensor/hub height elevation is found.

Kjeller Vindteknikk has developed the IceLoss model, Chapter 4, in which data from a NWP model is used in combination with an ice accretion model. As input to the model either pre-construction on-site measurements or parameters derived from operational data can be used. The result is site specific long-term ice loss estimations. A comparison with operational data is found in Chapter 5. The IceLoss model is only considering the average turbine elevation in the wind farm. It is assumed that less icing on turbines on low elevation sites are compensated by more icing on turbines at high elevation sites. One of the objectives in this project is to identify limitations in the existing methods and suggest and implement improvements in the IceLoss model. Based on operational data, the icing losses in WF1 and WF3 are showing clear positive height dependence. Thus, to get a more physical sound distribution of the ice load for large and more complex wind farms the individual turbine elevation should be considered. The development of the IceLoss model is described in Chapter 4 and results are presented in Chapter 5.

There are also examples of artificial neural networks in combination with mesoscale model data (Söderberg & Baltscheffsky, 2014), being used in estimating icing losses. The available methods can be used to estimate both long- and short-term icing losses.

Within the project "Large scale, cost effective wind energy development in icing environments" [2] several methods are developed by different participants. Leading

[2] The Swedish Energy Agency, D.nr.: 2009-001838, Project nr. 31464-2. Title: Large scale, cost effective wind energy development in icing environments

Edge Atmospheric have used surface observations, satellite images and NWP data to calculate icing rates and ice loads. The Swedish Meteorological and Hydrological Institute, SMHI, has within the project developed a method that is similar to the KVT IceLoss model, but based on other sources of NWP data.

VTT Technical Research Centre of Finland has developed a model where NWP data is used as input to an icing model that can be used to create icing climatologies. The model also includes a module that can simulate the ice accretion on the individual blades. The aerodynamic properties of the iced blades can then be studied with CFD analysis. The performance of a wind turbine with different ice loads / ice conditions on the blades can then be studied using other modules (Turkia, Huttunen, & Wallenius, 2013).

The simple methods, not involving NWP and ice accretion models are attractive due to its simplicity. However, they cannot describe condensation and precipitation processes and how icing is influenced by the regional topography. This is, at least to some degree, captured by the NWP models. Hence, the local effects are better described by the more advanced methods.

3.3 DESCRIPTION OF METHODOLOGIES FOR ESTIMATION OF SHORT-TERM ICING LOSSES OF OPERATIONAL WIND FARMS

Short-term estimations of the turbine ice load in a wind farm, icing forecasts, are made with NWP models. Typical forecast lead times are 24-48 hours. The icing forecasts are normally tuned with operational data from the wind farm. Real-time analysis of operational data, including detection of ice on the turbines, can also be used to improve the daily forecasts used in operational planning and energy trading. This is described in Chapter 6.

A brief overview of icing forecasts is found in Section 3.3.1. Additional information can be found in (Cattin, 2012).

3.3.1 Icing forecasts

Useful icing forecasts, capable of capturing variations and changes during the forecast period, are made using NWP models. The NWP models provide basic weather forecast data which is used as input to an ice accretion model in order to simulate ice loads. The end result is an energy forecast for the next couple of days adjusted for losses due to atmospheric icing.

The methodology is more or less identical to how NWP-based icing climatologies are made (Chapter 3.2.1) with the difference that icing climatologies use re-analysis data as input to the NWP model while (near) real time weather observations are, after post processing, used as input to the icing forecasts.

Kjeller Vindteknikk is using the Weather Research & Forecasting (WRF) model as input to the IceLoss model (Chapter 4) to produce icing forecasts. An evaluation of the performance of the IceLoss model used for forecasts is described in Chapter 6. Chapter 6 also includes results from development of the IceLoss model to include real-time operational data, aiming at improving the forecasts.

4 Description of the IceLoss model and developments made in this project

This section gives a description of our setup of the WRF model (Chapter 4.1) and the calculations of icing (Chapter 4.2) which has been used in the analysis in this project. Chapter 4.3 gives a description of how production losses have been estimated and Chapter 4.4 describes how the forecasts have been generated. Finally, Chapter 4.5 contains information about the developments made to the IceLoss model in this project.

4.1 MESO-SCALE MODEL DATA

The Weather Research and Forecast (WRF) model is a state-of-the-art meso-scale numerical weather prediction system, aiming at both operational forecasting and atmospheric research needs. A description of the modelling system can be found at the home page http://www.wrfmodel.org/. The model version used in this work is v3.2.1 described in Skamarock et al. (2008). Details about the modelling structure, numerical routines and physical packages available can be found in for example Klemp, Skamarock, & Dudhia, 2000 and Michalakes, o.a., 2001. The development of the WRF-model is supported by a strong scientific and administrative community in U.S.A. The number of users is large and it is growing rapidly. In addition the code is accessible for the public.

The geographical input data is from National Oceanic and Atmospheric Administration (NOAA). The data includes topography, surface data, albedo and vegetation. These parameters have high influence for the wind speed in the layers close to the ground. Surface roughness and landuse have been updated from Lantmäteriets GSD database in Sweden and from the N50 series from Kartverket in Norway.

The model setup used for this analysis is shown in Figure 4-1.

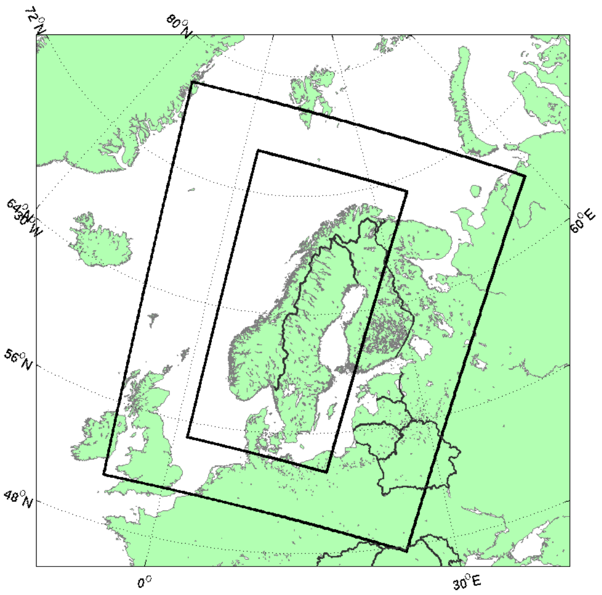

Figure 4-1 Model setup for the simulations used. The simulations has been carried out with a horizontal resolution of 4 km x 4 km for the inner domain shown.

The area covered by 4 km x 4 km resolution is given as the inner domain in Figure 4-1. The outer domain has a resolution of 16 km x 16 km. The meteorological boundary data used for this model setup originates from Final Global Data Assimilation System (FNL) available from the National Centres for Environmental Protection (NCEP) with 6 hours interval.

For the forecast simulations we have used the same model setup as used for the hindcast runs, shown in Figure 4-1. The boundary data used for the forecasting is from the GFS (Global Forecast System), available every six hours from NCEP (National Centers for Environmental Prediction).

Both simulations are setup with 32 layers in the vertical with four layers in the lower 200 m. We have used the Thompson microphysics scheme (Thompson, Rasmussen, & Manning, 2004) and the Yonsei University Scheme (Hong, Noh, & Dudhia, 2006) for boundary layer mixing.

4.2 ICE LOAD CALCULATIONS

According to the standard ISO 12494 icing has been calculated from

$$\frac{dM}{dt} = \alpha_1 \alpha_2 \alpha_3 \cdot w \cdot A \cdot V \tag{1}$$

Here dM/dt is the icing rate on a standard cylindrical icing collector (defined by ISO 12494 as a cylinder of 1 m length and 30 mm diameter), w is the liquid water content (LWC), and A is the collision area of the exposed object. V is the wind speed and α_1, α_2 and α_3 are the collision efficiency, sticking efficiency and accretion efficiency, respectively.

Periods of active meteorological icing is identified from the model data when the icing rate (dM/dt) exceeds 10 g/hour. The number of hours where active icing is identified is reported as "icing hours". 10 g of ice on the standard cylindrical icing collector is equivalent to a 0.5 mm layer of ice on the cylinder.

Accumulated over time equation (1) gives M as the mass of ice on a standard cylindrical icing collector. Icing is calculated at a specific height equivalent to the elevation of the turbine hub. The ice will often be left over some time after the period with active icing, until it disappears through shedding processes including melting or sublimation. The time periods when ice is present on the cylinder, are defined as periods with instrumental icing. Wind measurements are typically influenced by icing during these periods. In these periods there will typically be ice on the blades of the wind turbines resulting in a reduced power production. We have defined the periods with instrumental icing as the periods when the ice mass, M, exceeds 10 g/m.

There are several sources of uncertainty in the model data. The cloud processes are simplified and calculated by using parameterizations. Uncertainties therefore exist in the total amounts of cloud water available in the air masses, and in the distribution of cloud water vs. cloud ice in the air masses. The model setup is using the Thompson Microphysical Scheme which is recommended for liquid water content calculations.

Uncertainties are also related to the vertical distribution of the moist air and choice of parameterization scheme for the boundary layer mixing processes.

In the simulations the topography is represented by a grid, and does not reflect the real height of the mountain peaks. This means that the mountain tops in the model often are lower than in the real world. This discrepancy can lead to an underestimation of the icing amounts particularly for coarse model grids. The discrepancy in height is corrected for by lifting the air in the model to the correct terrain height. This lifting will contribute to lower the pressure and temperature in the air, and will lead to condensation in the cases when the air will reach the water vapor saturation pressure. The lifting is performed according to the vertical profile of temperature and moisture locally in the model.

4.2.1 Removal of ice

Ice melting is calculated by evaluating the energy balance model, given by

$$Q = Q_h + Q_e + Q_n, \qquad (2)$$

where Q_h and Q_e are the sensible and latent heat fluxes. Q_n is the net radiation term. There are also other terms in the total energy balance model, however they are assumed to be of negligible size in this context. A detailed description of the melting terms is given in (Harstveit, 2009).

When Q becomes positive, melting will start. Often during melting episodes, the ice does not melt gradually away such as described by the energy balance model. When the melting is initialized the ice will fall off more quickly by shedding, particularly from a rotating blade. This ice shedding is a stochastic process which makes it difficult to estimate the time when all ice is removed. In this work no ice shedding is assumed in relation to melting of the ice. The melting process is found to happen quite quickly in the model. A shedding factor would further speed up the process. This implies that the ice load can be overestimated at some periods during melting. The melting process does however happen quite fast, so only shorter periods of time will be affected.

Sublimation is a process for ice removal that is found to be important, in particular for dry inland sites where the temperature can stay below freezing for several months continuously during the winter. At such sites the accumulated ice will not melt. Sublimation is defined as the transfer of ice from solid state directly to water vapor. This will happen in situations with dry and cold air. The sublimation rate increases with wind speed when the ventilation of the iced object is high. This can allow for faster ice removal of a rotating turbine blade compared to a fixed object. The sublimation rate is calculated by evaluating the energy balance between outgoing long wave radiation and latent heat release from the sublimation process. Sublimation has been included in the icing calculations. During the process of sublimation we have observed (from web cam images) that the ice becomes brittle and that small pieces of ice continuously fall off the cylinder. This shedding is included by multiplying the sublimation rate with a factor of 2.5.

4.3 PRODUCTION LOSS ESTIMATE

To estimate the production loss we assume that the energy production will continue with ice on the rotor blades. Ice on the blades will disrupt the aerodynamic structure of the blades which leads to a lower energy yield. The energy production follows the principle of a two parameter power curve as shown in Figure 4-2. The two parameter power curve was developed from the operational production data from several Swedish wind farms in the project "Large scale, cost effective wind energy development in icing environments" [3]. Not all turbines continue to operate with ice on the blades. If the turbines are stopped during icing, that must be considered in the loss estimation. The importance of considering the operational strategy is further discussed in chapter 5.3.1.

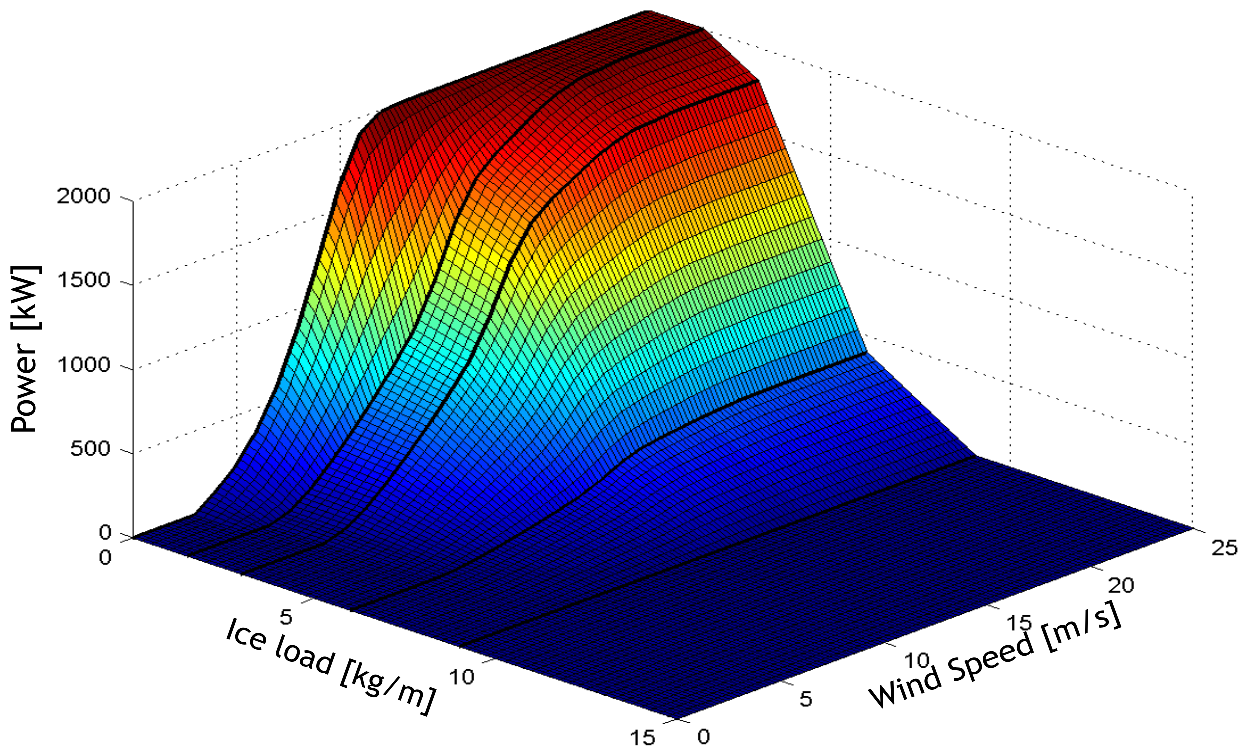

Figure 4-2 Two-parameter power curve *P(V,M)*, function of ice load and wind speed.

4.4 FORECASTING OF POWER PRODUCTION AND ICING

The modelled data for each wind farm have been statistically tuned toward observed nacelle wind speeds. We have calculated a set of transfer coefficients to relate the wind speed given by the WRF model to the nacelle anemometer for each of the turbines.

Tuning coefficients for each of the wind farms have been generated and used for the forecasting of the energy production for individual turbines in each wind farm. The transfer coefficients are given as sector vise values for 12 direction sectors. In this way we are able to include wake effects in the wind farm in the WRF model data. By using

---

[3] The Swedish Energy Agency, D.nr.: 2009-001838, Project nr. 31464-2. Title: Large scale, cost effective wind energy development in icing environments

individual power curves for each turbine we are able to give a power forecast for each turbine for clean blades.

The icing rate (eq. 1) has been calculated for each forecast simulation. The IceLoss model requires, however, also ice load as an input. The forecasted ice load from the previous forecast run has thus been used as an initial condition, using the time step corresponding to the initial time step of the new forecast run. The production loss due to icing has been estimated in the forecast using the two parameter power curve described in Chapter 4.3. Developments of the methodology to use operational data to estimated the initial ice load in the wind farm is presented in Chapter 4.5.

4.5 DEVELOPMENTS OF THE ICELOSS MODEL IN THIS PROJECT

4.5.1 Height dependent calculations – IceLoss_elev

The original IceLoss model is using the average turbine elevation in the calculations. It is assumed that less icing on turbines on low elevation locations are compensated by more icing on turbines at high elevation locations. The results in Chapter 5 show that this is a good assumption. However, for wind farms with a wide range of turbine elevations and when the distribution of turbine elevation is not symmetric around the mean it is expected that the assumption is less valid. A calculation that considers the individual turbine elevation is a first step towards the possibility to make more detailed evaluations of the distribution of ice within the windfarm. But, as presented in Chapter 5.4.1, there are several factors that affect the icing within the wind farm that is still not considered in the IceLoss calculations.

The development of IceLoss to consider the individual turbine elevations is quite straight-forward. The calculation of the atmospheric parameters relevant for icing, as described in Section 4.2 is made to the individual turbine elevation and hub height, instead of using the average turbine elevation with the average hub height. Hence, the physics in the model is not changed or developed.

4.5.2 Initial ice loads in forecasts

One major challenge in the forecasting of energy from a wind farm during the cold season is how to estimate losses due to ice. The ice load on the turbines in combination with wind speed is used in the two-parameter power curve, Figure 4-2, to get the production when there is ice on the blades. The initial ice load is based on the last forecast, Section 4.4. An improvement to this would be to use the actual ice-situation in the wind farm as initial ice load. This requires access to SCADA data in (near) real-time. It should in general not be too difficult to arrange a technical platform, such as an ftp-server, where data could be shared between the wind farm owner and the forecast provider.

The implementation should be rather straight forward, instead of looking for ice in the last forecast, the SCADA data is analyzed as described in section 5.1.1. Based on this, the turbines affected by ice can be identified. Using the produced power and the wind speed during the icing periods, the ice load can be estimated from the two-parameter power curve in Figure 4-2. First one must have a criterion for when the wind farm is said to be affected by icing. One suggestion is "Icing is said to affect the wind farm if at least 50 % of the 10-minute time steps during six hours before the forecast start time is flagged as ice for at least 50 % of the turbines".

The ice load should then be set to 0 if no ice is detected in the wind farm, and the initial ice load in cases of ice in the wind farm should be adjusted based on the observations. The results of initial tests have not provided significant improvements in the forecasts. It seems to be rather difficult to determine the correct ice load based on the observations and. Since this is not in the core scope of the project, it is not developed further. Instead this is proposed for future work.

5 Post-construction estimation of icing losses

This chapter describes the methodology and the results when estimating the production loss due to icing based on measurements and modeled data.

5.1 METHODOLOGY

5.1.1 Operational data

Median power curves have been calculated using the median power values for wind speed bins at every 0.5 m/s (Figure 5-1). Prior to calculating the median power curves, the following data are filtered out:

- Data with an alarm code, along with the time step after the alarm occurred.
- Data for periods with curtailed power output.
- Data that may be affected by icing, WRF temperature < 3 ºC [4].
- Occasions when the nacelle wind speed is more than two meters above cut-in and the power production is less than 5 kW.

In addition, for each turbine, threshold power curves based on the 10-percentile power value in each wind speed bin are defined (Figure 5-1). When the power from the turbine is below the threshold power curve, the period is flagged to be affected by icing given that the operational codes also indicate normal operation and that the temperature from WRF is below 3 ºC. Only indications that are lasting more than 3 consecutive time steps are considered to be icing events.

Power curves for one year periods are calculated to avoid seasonal bias. It is also wise to not use too long periods since changes can be made to the turbines during the time of operation. The power curves are used to detect ice during their respective year. Tests have been made to make a second set of power curves after ice filtering. Now occasions with temperature below 3 ºC are included if they are not flagged to be affected by icing. This will include more winter data in the derivation of the median power curves. However, it is found that there only is a small difference compared to the original set of median power curves for the wind farms included in this project. The median power curves based on the filter settings above are used throughout the report if not stated otherwise.

[4] The temperature used to define periods not affected by icing is from the KVT Meso dataset. The modeled temperature is used instead of temperatures measured by the turbine because we have no knowledge about the location of the temperature sensor; the heat from the nacelle can create a bias.

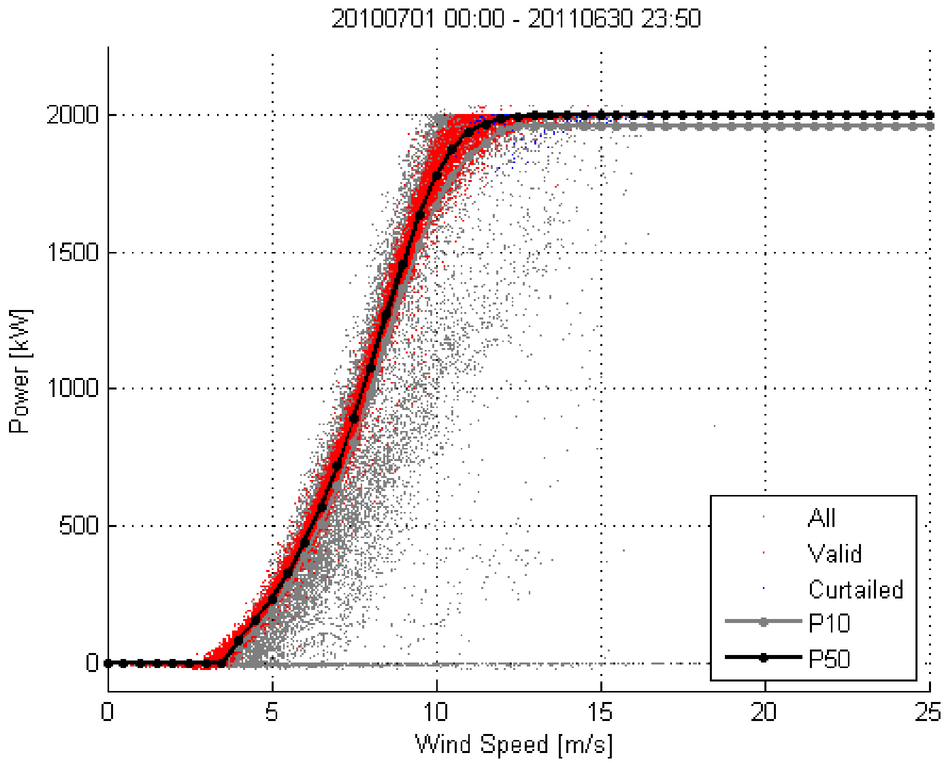

Figure 5-1: Observed wind speed versus power for one WF1 turbine for a 12-month period. Grey, red and blue points indicate all, valid and curtailed data, respectively. The amount of curtailed data is very small and disappear among the grey points. Black and gray line indicates median and 10th percentile power curve based on filtered (valid) data and with a velocity bin resolution of 0.5 m/s.

The operational production loss due to icing is calculated as the aggregated difference between the actual production during periods flagged as icing periods and the expected production for the turbine with respect to the yearly production.

The expected production is calculated using the methods PEP-PC1 and PEP-PC2. They are described in short below, more information can be found in (Lindvall, Hansson, & Undheim, 2016). The other PEP-methods described in (Lindvall, Hansson, & Undheim, 2016) all require one or more turbines not affected by ice available as reference. This is rarely the case during icing conditions.

Description of PEP-PC1

The basis for this method is to define specific power curves for each WTG based on the nacelle wind measurements and the actual production for the periods when the WTG is in full performance. To estimate PEP for occasions when turbines are not running in full performance the measured nacelle wind speeds are applied to the derived power curves.

Since the PEP-PC1 method relies on the wind speed measured at the nacelle it is important that the quality of the data can be assured, and that no unknown major revisions have been made to the nacelle transfer functions during the period investigated.

In theory the derivation of specific power curves could be based on Wind Iris measurements instead of nacelle anemometer measurements. This would be highly impractical since the Wind Iris would need to measure at many turbines for long periods of time in order to get a sufficient amount of data in order to derive the power curves. The lidar would also need to be installed at the turbine(s) during the period when losses are estimated. This is not realistic in a commercial project.

Description of PEP-PC2

In this method modeled WRF wind data and the actual production data for WTGs running in full performance is used to derive specific power curves for each WTG. Considering that the modeled wind speed is not influenced by wake effects, the specific power curves are derived with respect to the wind direction to account for wake effects.

For periods when a WTG is identified not to be running in full performance the PEP is calculated by applying the modeled WRF wind speed and wind direction to the derived specific power curves of that WTG.

5.1.2 Modeled data (IceLoss)

The IceLoss model is presented in Chapter 4. Operational wind farm data is used as input to the IceLoss model. Wind speed and wind direction data is used to scale the model data. To account for differences in wake effects between different turbines, a set of transfer coefficients relating the wind speeds given by the numerical model WRF to the nacelle anemometer for each of the turbines are calculated. The transfer coefficients are given as sector-wise values for 12 direction sectors. The transfer coefficients are the slope and offset from a linear fit to the relation between observed and modeled wind speeds.

The power curves from the same period as the transfer coefficients are calculated, Section 5.1.1. The power curves are not calculated sector-wise. It is seen that the difference between sector wise power curves and the power curves containing all data is small, see (Lindvall, Hansson, & Undheim, 2016) In the calculation of the power curves, the nacelle wind speeds have been adjusted for varying density according to (IEC 61400-12-1, 2005).

There will be differences in the transfer coefficients due to the year-to-year variability of the wind. A sensitivity test is therefore performed using data from WF1. Transfer coefficients for all periods to the left in Table 5.1 are calculated. The IceLoss model is then run eight times, applying the different transfer coefficient – power curve pairs on WRF data from the period 2000 – 2014. The result is eight different calculations of hub height wind speed. The eight wind speeds differs rather much depending on whether the transfer coefficients are based on data from before or after the revision of the NTF (nacelle transfer function) mentioned in Section 2.1.2. However, the difference in estimated relative production loss due to ice is very small regardless if transfer coefficients and power curves from before or after the revision are used. Thus, the IceLoss calculation is robust with respect to erroneous nacelle anemometer measurements, as long as the used transfer coefficients and power curve are based on the same data set. This robustness is also indicating that the derivation of transfer coefficients and median power curves based on Wind Iris measurements instead of nacelle anemometer measurements would be of little benefit. The Wind Iris would also need to measure at many turbines for long periods of time in order to get a sufficient amount of data. This is not realistic in a commercial project.

For a fair comparison between the operational and modeled data it is important to carry out the same filtering for both datasets. Therefore, periods with invalid or missing operational data are also removed from the WRF dataset. In addition, all the periods when the operational power data has an alarm or curtailed power is filtered out from the WRF data. The power loss due to icing from the WRF model is the aggregated difference between the full production based on the modeled wind speeds and the modeled ice-reduced production described in Chapter 4 during the periods when no alarm or curtailment are identified as described above.

5.2 RESULTS WF1

For each of the 17 turbines, power curves representative over one year periods, as defined to the left in Table 5.1, have been calculated from the nacelle anemometer and power data. The calculated power curves from the individual turbines within a period are found to be similar. The NTF, describing how the wind measured by the anemometer on the nacelle is adjusted to represent the undisturbed wind speed ahead of the rotor, was revised during spring 2010. The calculated power curves **before** and **after** the revision differs. The revision is the reason for the partly overlapping periods in the beginning. To have a large enough data set to calculate the power curve from, one year periods are used. The same holds for the end of the period. We have tried to avoid splitting a winter season on different years, hence the periods break in the summer.

Table 5.1. Periods when power curves are calculated are to the left. Periods when the power curves are used to identify icing are to the right.

PC calculation period	PC used on period
2009-03-01 - 2010-02-28	2009-03-01 - 2009-06-30
2009-05-01 - 2010-04-30	2009-07-01 - 2010-04-30
2010-05-01 - 2011-04-30	2010-05-01 - 2010-06-30
2010-07-01 - 2011-06-30	2010-07-01 - 2011-06-30
2011-07-01 - 2012-06-30	2011-07-01 - 2012-06-30
2012-07-01 - 2013-06-30	2012-07-01 - 2013-06-30
2013-07-01 - 2014-06-30	2013-07-01 - 2014-06-30
2013-10-01 - 2014-09-30	2014-07-01 - 2014-09-30

5.2.1 Icing losses, period of operation

Following the methodology described in Chapter 5.1, operational icing losses and IceLoss data have been estimated for the period July 2009 to June 2014. We have divided the period into winter years. A winter year is defined as the time period between July 1st and June 30th in order to avoid splitting up the winter season into two consecutive years.

Figure 5-2 shows the calculated annual icing loss values for the operational data and from IceLoss. The relative values are given with respect to the expected energy production. The figures above the bars in Figure 5-2 are indexes that provide information about the production each year with respect to the average of all years (index 100). The index is based on the full dataset of PEP-PC2. As described in Section 5.1, periods with operational alarm data have also been filtered out from the WRF data to make a fairer comparison between the measurements and the model. The period 2011-07-01 – 2012-06-30 is used to derive the power curves and transfer coefficients for the IceLoss model. As mentioned, the difference between individual years is small and either of the periods could have been chosen, producing similar results. Results both from the original IceLoss and IceLoss_elev (described in Chapter 4.5.1) are shown in Figure 5-2. The difference between the two versions of the model is small. This is a good indication of that the assumption used in the original model setup, less icing on turbines on low elevation locations are compensated by more icing on turbines at high elevation locations, is valid and working. Larger differences between the model versions are expected for wind farms where the range in turbine elevation is larger and where the distribution of the turbine elevations is not symmetric around the mean. The version with individual calculations will also provide a possibility to investigate the distribution of icing within the wind farm.

It must be noted that the nacelle anemometers, used in PEP-PC1, are scaled to represent the upstream wind velocity. These scaling parameters will be valid when the turbine is in operation and producing power according to its power curve. Ice on the rotor will change the friction that the wind experiences. The rotational speed of the rotor might also be affected and this can cause the measured wind to be incorrectly scaled. Thus, PEP-PC1 might be less suitable for the estimation of icing events. PEP-PC2 might therefore provide a better estimation. According to (Lindvall, Hansson, & Undheim, 2016) the bias is less for PEP-PC2 compared to PEP-PC1 while the mean absolute error is less for PEP-PC1 compared toPEP-PC2. Looking at averages over long periods of time, a low bias is preferred.

The estimated total ice loss values both for the period 2009 to 2014 and for the average of all periods show good agreement between the operational and modeled data. However, the relative differences can be considered large for some years. It is for example close to 50 percent during the winter year 2011-2012, Figure 5-2. The IceLoss estimations are in general showing the highest losses. The IceLoss model indicates that for WF1 the five winter seasons covered by operational data experienced larger losses due to icing than normal. The normal values are based on model results from the period 2000-2014. Given that the operation strategy to icing will remain unchanged during the lifetime of the wind farm we have reason to believe that a smaller loss due to icing than experienced is expected.

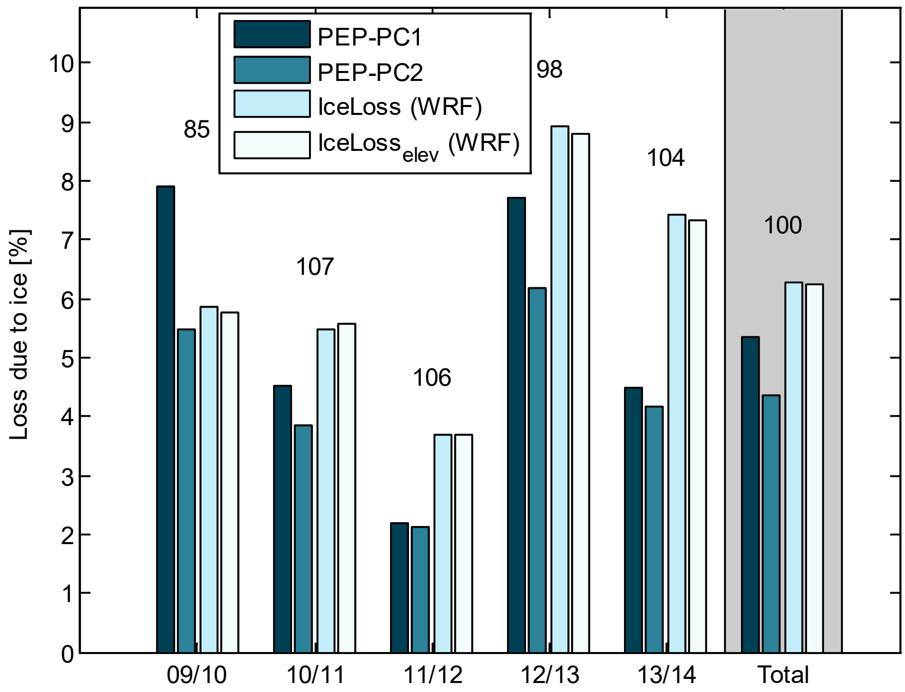

Figure 5-2 The estimated energy loss due to icing for WF1, based on operational and modeled data. The figures above the bars are an index that provide information about the production each year with respect to the average of all years (index 100). The index is based on the full dataset of PEP-PC2.

On turbine level we see, as expected, that higher turbine elevation gives a higher loss due to icing. The individual turbine loss versus height, based on operational data, is found in Figure 5-3 and we see clear positive linear trends for all years and the slopes of the linear trends are similar for all years. The losses are derived using PEP-PC1. The scatter is rather large for some of the years. The scatter reflects the uncertainty in the detection of icing in the operational data. Another possible factor contributing to the scatter is sheltering effects within the wind farm. Sheltering effects are studied for WF3 in Chapter 5.3.

In Figure 5-4 icing loss results from individual turbines based on the original IceLoss model is shown. The height dependence is less clear, this is not a complete surprise since models are simpler and smoother than the real world and therefore cannot capture all variations. The height dependence that is present in the model data is due to scaling of the model wind speed against the wind speed measured by the nacelle anemometers. The wind speed is linearly related to the calculated ice load and the fact that the wind speed is higher at higher elevations is causing the height dependence in the model. There is however one year when the icing losses seem to decrease with increasing elevation. The cause of this can be the scaling coefficients relating the model wind speed and the measured wind speed at the turbines (see the top in section 5.1.2). The coefficients depend on the data availability during the year, and lack of data and erroneous values that has managed to slip through the filters can be responsible for this behavior.

The results from IceLoss_elev, described in Chapter 4, are shown in Figure 5-5. All years are now showing positive height dependence, making it more physical sound, although the slopes are less than those found in operational data.

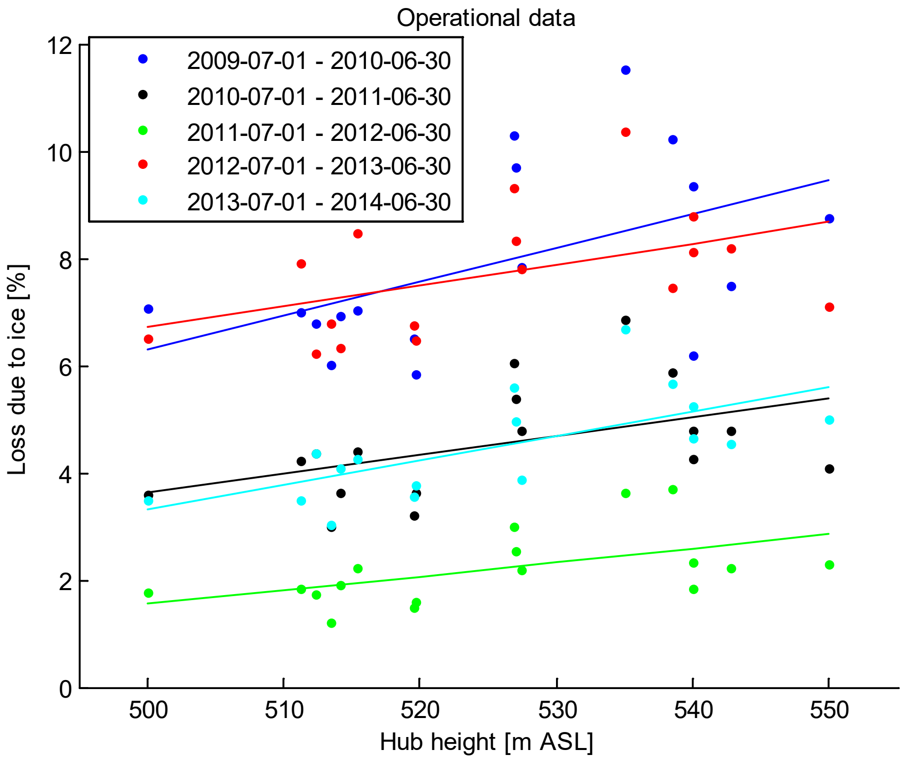

Figure 5-3. The dots represent the yearly loss from individual turbines in WF1, based on PEP-PC1. A linear fit to the losses vs. height each year is included to highlight the trends.

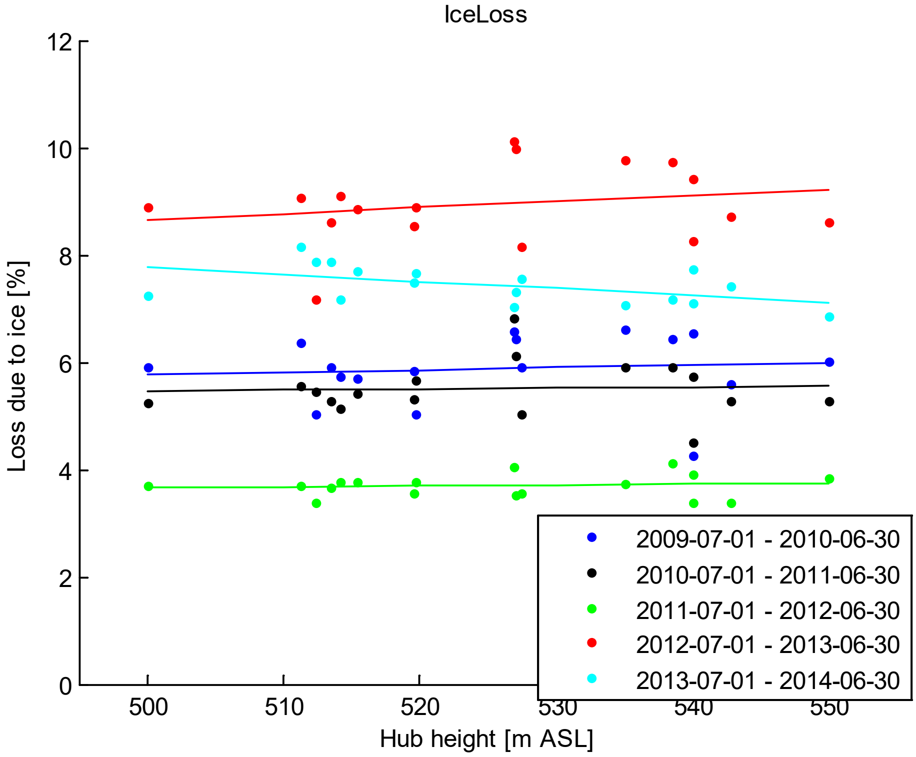

Figure 5-4. The dots represent the yearly loss from individual turbines in WF1, based on the IceLoss model run with median power curves and wind transfer coefficients based on operational data. The mean wind farm elevation and hub height is used in the calculations. A linear fit to the losses vs. height each year is included to highlight the trends.

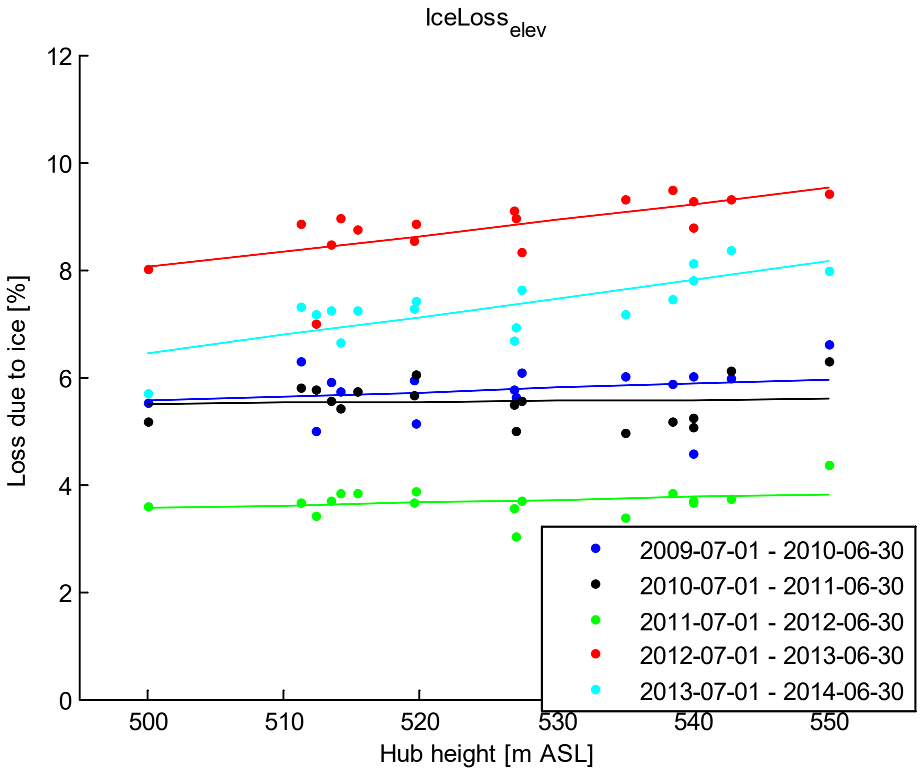

Figure 5-5. The dots represent the yearly loss from individual turbines in WF1, based on the IceLoss model run with median power curves and wind transfer coefficients based on operational data. Individual turbine elevation and hub height is used in the calculations. A linear fit to the losses vs. height each year is included to highlight the trends.

5.2.2 Time series comparison

From the previous section it is clear that the IceLoss model is doing a good job estimating icing losses when looking at averages over several years. It is also interesting to compare time series of modelled ice load and the presence of ice in the SCADA data. Three examples are found in Figure 5-6, Figure 5-7 and Figure 5-8. It is seen that occasions when the model predicts large ice loads corresponds well with ice detected in the SCADA data. Figure 5-8 show periods when the model has no or only small ice loads while the majority of the turbines are classified as affected by ice based on the SCADA data. The data flagged as affected by ice in March 2013 for one turbine are shown with the median power curve and the threshold power curve used for detection of ice in Figure 5-9. It is seen that the majority of the data flagged as affected by ice is just below the threshold power curve. This means that the production loss is relatively small. It also indicates that the icing situations are weak and perhaps not always captured by the IceLoss model. There is of course also an uncertainty in the detection of icing in the SCADA contributing to the result.

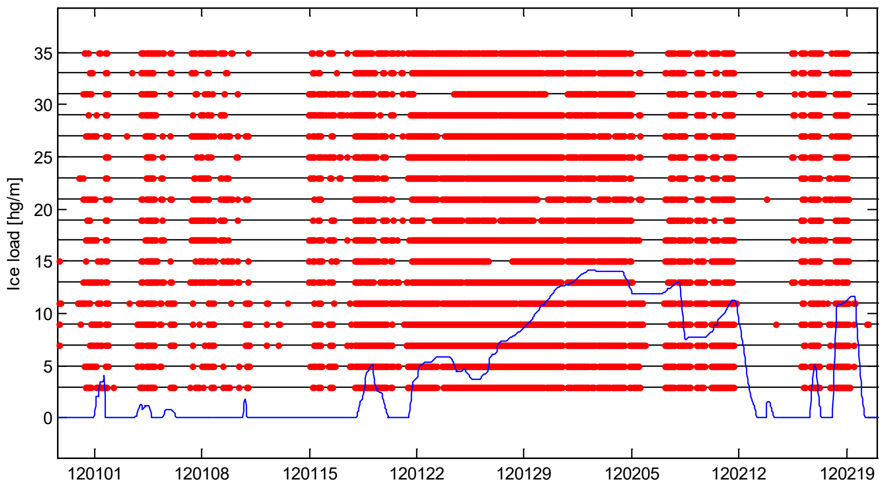

Figure 5-6. The blue line is showing the modelled ice load during part of January 2012. The lines are representing the turbines in WF1, separated vertically for readability. The red is indicating when ice is detected in the SCADA data.

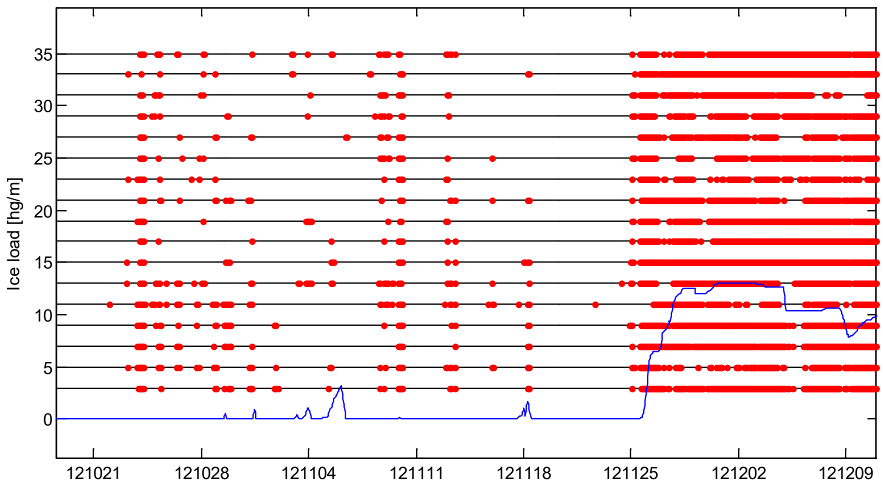

Figure 5-7. As Figure 5-6 but for a period in November-December 2012.

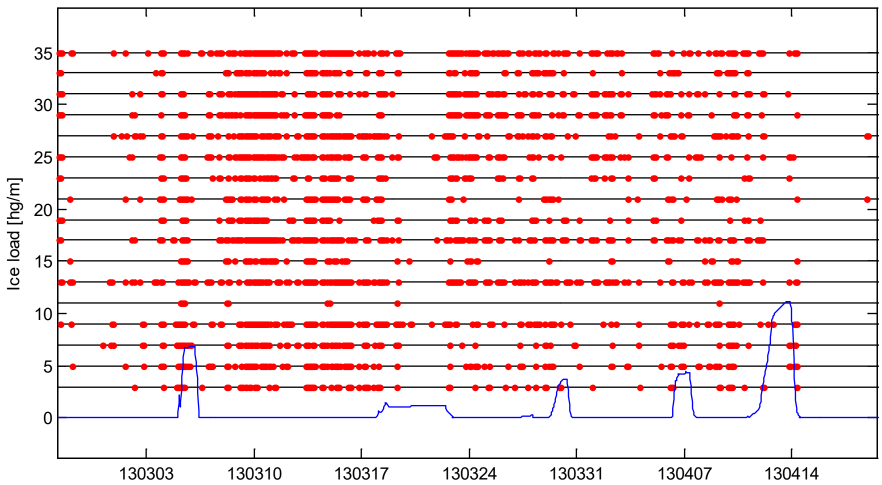

Figure 5-8. As Figure 5-6 but for a period in March 2013.

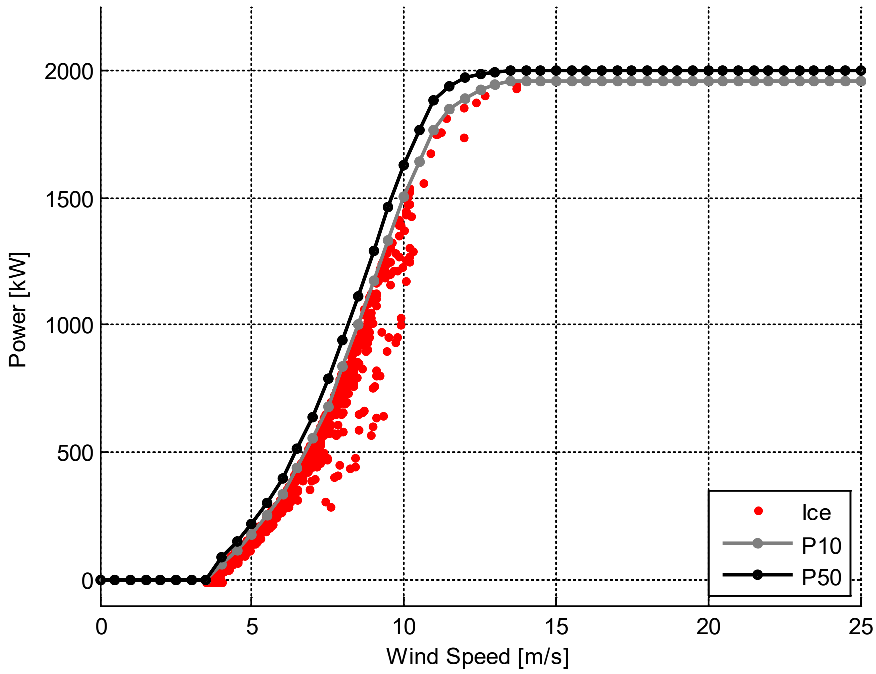

Figure 5-9. Median power curve (P50), threshold power curve used for detection of ice (P10) and data flagged as iced during March 2013 for one turbine.

5.3 RESULTS WF2

For each of the turbines, median power curves representative for one year periods, as defined to the left in Table 5.2, have been calculated from the nacelle anemometer and power data. See section 5.1 for more information about the methodology. A comparison of the power curves from the different turbines in each period show only small variations.

Table 5.2. Periods when power curves are calculated for WF2 are to the left. Periods when the power curves are used to identify icing are to the right.

PC calculation period	PC used on period
2012-06-01 - 2013-03-31	2012-06-01 - 2013-03-31
2013-04-01 - 2014-03-31	2013-04-01 - 2013-05-31
2013-06-01 - 2014-05-31	2013-06-01 - 2014-05-31

Power curves and wind transfer coefficients from the period 2013-06-01 – 2014-05-31 are used in the PEP methods and in IceLoss. The yearly losses (winter years) are found in Figure 5-10. The relative values are given with respect to the expected energy production. The figures above the bars are an index that provides information about the production each year with respect to the average of all years (index 100). The index is based on the full dataset of PEP-PC2. The agreement between IceLoss and the PEP-methods is poor, the reason for this is investigated in section 5.3.1. Results both from the original IceLoss and IceLoss_elev are also shown. The difference between the two IceLoss configurations is small, indicating that the assumption used in the original model setup, less icing on turbines on low elevation locations are compensated by more icing on turbines at high elevation locations, is valid and working. See also Chapter 4 and Chapter 5.2.1. The IceLoss model indicates that for WF2 the two winter seasons covered by operational data experienced smaller losses due to icing than normal. The normal values are based on model results from the period 2000-2014. Given that the operation strategy with respect to icing will remain unchanged during the lifetime of the wind farm we have reason to believe that a larger loss due to icing than experienced is expected.

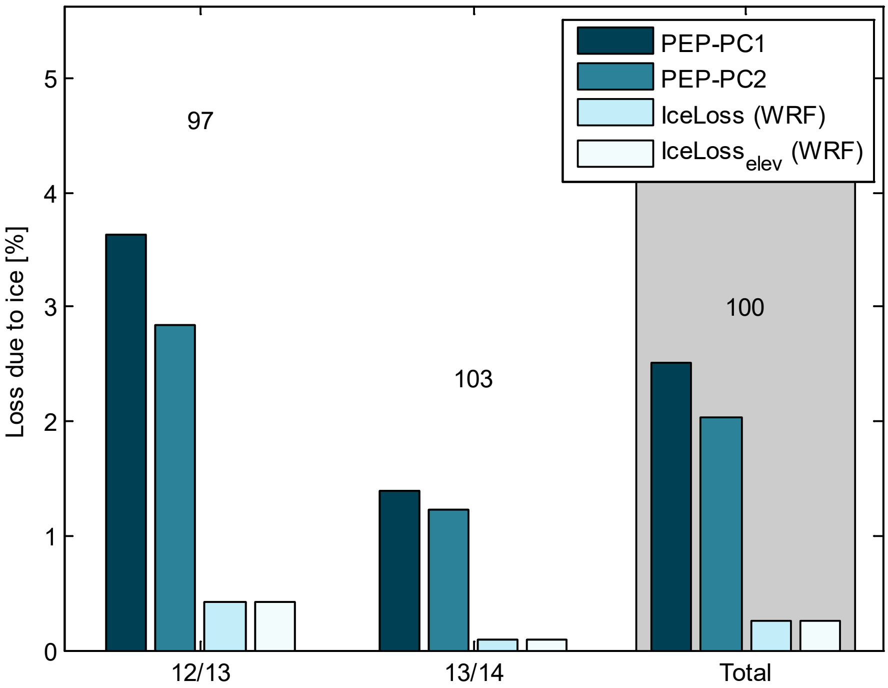

Figure 5-10. The estimated energy loss due to icing for WF2, based on operational and modeled data. The figures above the bars are an index that provide information about the production each year with respect to the average of all years (index 100). The index is based on the full dataset of PEP-PC2.

5.3.1 Analysis of turbine behavior

The agreement between the IceLoss model and the losses due to ice based on operational data is poor, Figure 5-10. The causes for the bad agreement between IceLoss and the operational data for WF2 can be related to

1. Model uncertainties and model errors

Numerical modeling is always associated with uncertainties; it is not possible to exactly describe the complex turbine-atmosphere system. There are also assumptions made in the IceLoss calculations that might not be valid for all wind farms.

2. Errors in the ice detection filter routine

Ice on the turbines is detected with a threshold power curve, the ambient temperature and information of the turbine state, see section 5.1.1. As mentioned in section 2.1.5, the information about the turbine state code is limited for WF2. It is therefore possible that state codes identified as valid when the turbine is in full performance has been erroneously defined. There is also an uncertainty in the threshold power curve that fall into this category. The turbine regulation strategy can also be responsible for errors in the ice detection filter routine, read more below.

3. Turbine regulation strategy

If the turbine is shut down or regulated during icing occasions in a way that is not considered in the IceLoss model, the loss will be underestimated by the model. The observed losses due to icing from WF2 correspond well with modeled losses when it is assumed that the turbines are shut down when the modeled ice load is above 50 g/m. It is however not likely that the turbines actually are shut down/regulated during all such occasions since the regulation strategy can make data erroneously flagged as iced. This is most likely the case for WF2 since the filter routines also detects ice during the summer if the temperature constraint in the filter settings is disregarded. As described in section 5.1.1 ice is identified as occasions when the turbine is in a state identified as full performance, but with production less than the threshold power curve and with the requirement that the temperature is below 3ºC. Note that occasions with weak wind, below turbine cut-in, are disregarded in the detection of ice. One way to make the filters better could be to include more SCADA parameters as constraints. But if no details about how the turbine itself is detecting ice are known, it would still be difficult to actually know if it is ice or some other atmospheric/ambient conditions that is causing the turbine to regulate itself in a way that makes the power fall below the threshold power curve. High quality ice load measurements made with state-of-the-art instruments in the wind farm would be valuable in the investigation of the regulation strategy. The development of improved filters using ice load measurements is proposed for future work. It has been suggested by VTT Technical Research Centre of Finland Ltd that a lidar can be used to detect occasions with icing (Karlsson, Peltola, Antikainen, & Vignaroli, 2015). This is done by analyzing patterns in the backscatter signal from the lidar. This could be one way of increasing the knowledge about the specific turbine behavior during icing occasions. The VTT results are based on a ground mounted lidar. But the methodology might be applicable, with some modifications, also for nacelle mounted lidars. However, since the possibilities to validate the results based on only lidar and SCADA-data is limited it has not been investigated further. A validation would require ice measurements and preferably also information about the cloud base / type and real-time images from the site.

It seems quite clear that the turbines in WF2 are not operated as normal with ice on the blades. The top panel of Figure 5-11 shows the rotor RPM vs. wind speed during periods with full performance and during periods when ice is detected. The figure is based on data from one turbine but is representative for all turbines in WF2. The icing periods are split up in two categories: when the turbine state is X and when the turbine state is everything but X. Full performance state code for WF2 is not a single number, but a range (remember that we require a full performance state to detect ice). X is considered to be the normal state of the turbines. It is the dominating state making up the bulk of the data during icing events. X is also the most common code looking only at full performance episodes. The top panel in Figure 5-11 shows that the RPM seems to be curtailed to around 5 RMP for a large range of wind speeds. This is also confirmed by the histogram in the bottom panel of Figure 5-11 showing the distribution of the RPM during periods with full performance and during the two icing categories. The 5 rpm class is over-represented in the icing periods. It is not completely clear that it is icing that is causing the curtailment, but since it is not present during full performance events, and dominating in the X-ice periods it is likely that the turbine is detecting some anomaly during icing events and regulates itself. The difference in regulation strategy between the turbines in WF2 and WF1 can be seen in Figure 5-12. For WF2 the power curve during a winter period with a high frequency of iced data, considering only state X episodes but no other filters, is rather narrow. When ice is detected, the power is close to 0. Hence, the production is either close to the median power curve or 0. For WF1, where we know that the turbines are operated with ice on the blades, the power curve during the winter is wider. For WF1 we use only data without any alarm code. No other filters are applied on the data.

From this we can conclude that the assumption used in IceLoss, that the turbines continue to produce but with ice on the blades, is not valid for WF2.

The loss due to icing for WF2 is larger than expected for this part of Sweden. The control strategy is questionable. For wind farms in operation it is recommended to evaluate the turbine control strategies at regular intervals. It is also recommended that turbine control strategies during icing are discussed with the turbine manufacturer before any purchase to avoid unnecessary losses.

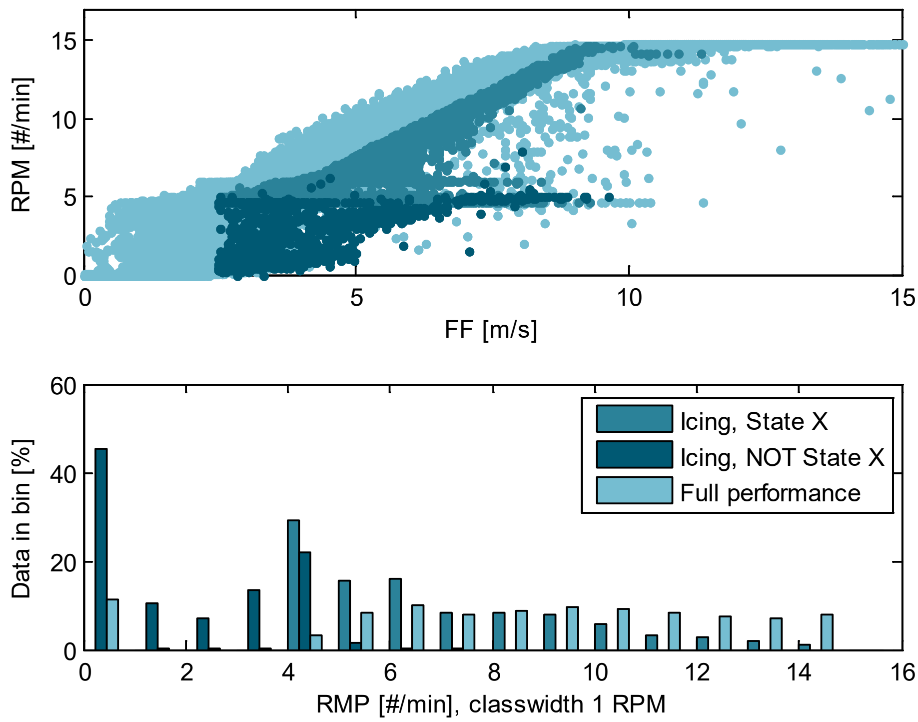

Figure 5-11. Top panel: Rotor RPM vs. wind speed for periods with full performance and during periods identified as affected by icing. The results are for one turbine. Read more about State X in the text. Bottom panel: The distribution of rotor RPM during full performance periods and during periods identified as affected by icing.

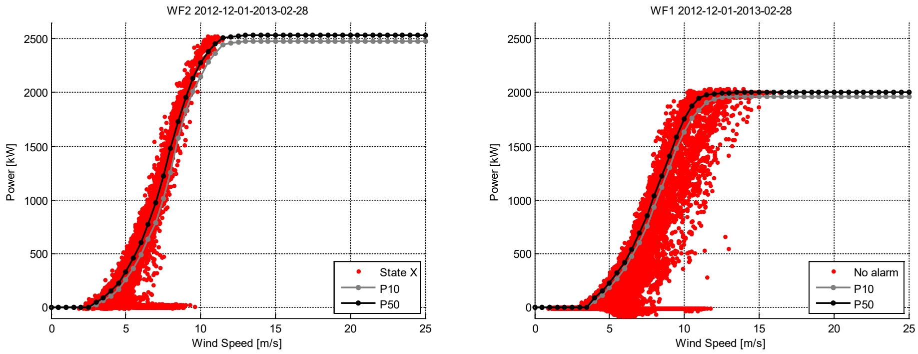

Figure 5-12. Examples of two different regulation strategies during the winter. Left: The WF2 turbines are shut down / regulated during icing events. The PC is close to the median power curve (narrow , red dots) during periods with normal operation while it is 0 during the regulation periods. All occasions with state X (read more in the text) during the period indicated in the figure title are shown in the plot. Right: The WF1 turbines are not regulated during icing events, instead they are operated with ice on the blades, making the PC broader. All occasions without any alarm is included in the plot, no other filters are applied on the data.

5.4 RESULTS WF3

Power curves used for ice detection are calculated for the periods in Table 5.3. For two of the turbines, the calculated power curves were unsuitable for ice detection. One possible cause for the failure to calculate a good looking power curve might be that the operating state from the turbine is set to "normal" even if it is not. However, no further analysis has been made to pin point the exact reasons for this. Instead an average of the other power curves for the same type of turbine has been used in the ice detection process for the two turbines. This approach will be good if the two turbines perform similar to the other turbines of the same type. If not, the ice detection might not capture ice affected data or might flag too many observations as affected by ice. In this case it is seen that using the average power curve from the other turbines are causing an overestimation in the number of icing events detected. Since it is only two turbines out of 40, the overall result will not be significantly affected. In situations with less turbines it could however have a significant effect, and then the recommendation is to not use the turbines.

Table 5.3. Periods when power curves are calculated for WF3 are to the left. Periods when the power curves are used to identify icing are to the right.

PC calculation period	PC used on period
2010-12-01 - 2011-12-31	2010-12-01 - 2011-06-30
2011-07-01 - 2012-06-30	2011-07-01 - 2012-06-30
2012-07-01 - 2013-06-30	2012-07-01 - 2013-06-30
2013-07-01 - 2014-03-18	2013-07-01 - 2014-03-18

The power curve and wind transfer coefficients for the winter period 2013-10-01 – 2014-03-18 are used in the PEP methods and in IceLoss. The yearly losses (winter years) are found in Figure 5-13. The index is based on the full dataset of PEP-PC2. There is good agreement between IceLoss and the PEP-methods. Results both from the original IceLoss and IceLoss_elev are shown. The IceLoss model indicates that for WF3 the four winter seasons covered by operational data experienced larger losses due to icing than normal. The normal values are based on model results from the period 2000-2014.

Given that the operation strategy to icing will remain unchanged during the lifetime of the wind farm we have reason to believe that a smaller loss due to icing than experienced is expected.

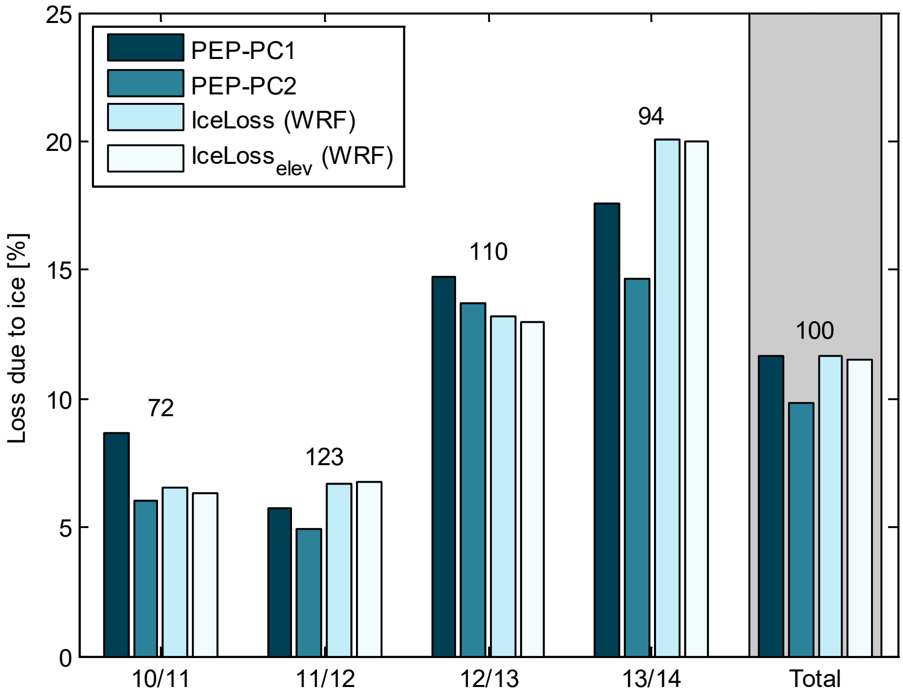

Figure 5-13. The estimated energy loss due to icing for WF3, based on operational and modelled data. The figures above the bars are an index that provide information about the production each year with respect to the average of all years (index 100). The index is based on the full dataset of PEP-PC2.

On turbine level we see, as expected, that higher turbine elevation gives a higher loss due to icing. The individual turbine loss versus height, based on operational data, is found in Figure 5-14 and we see clear positive linear trends for all years. The losses are derived using PEP-PC1. The slope of the fit to the individual turbine icing losses is not consistent between the individual years in Figure 5-14. The scatter is larger for the last two winters, showing similar slope. While the first two winters is having a rather different slope compared to the last years. Different climatic conditions and wind distributions during the different years could be responsible for this behavior. Possible sheltering effects, depending on the wind direction, will thus be different for different years. Sheltering is when turbines upstream in a wind farm will experience more icing than turbines downstream. More about sheltering effects in WF3 is found in Chapter 5.4.1.

In Figure 5-15 icing loss results from individual turbines based on the original IceLoss model, using the wind farm average elevation, is shown. The height dependence of the losses due to icing is negative for all the studied years. IceLoss_elev is making the slope more negative during one of the years, decreasing it for one year and making it positive for two years, Figure 5-16. The reason for the negative slopes is a combination of the uncertainty in deriving the wind transfer coefficients and the uncertainty in the WRF model. IceLoss_elev has also been run with estimated wind at the turbines from a pre-construction wind simulation made by the wind farm owner. The result is shown in Figure 5-17. Three of the years are showing similar, positive slopes, while one is still negative. The WAsP winds are of course associated with uncertainty, but they are consistent in the way that they, in this case, always are higher at higher elevation positions. Thus, using theoretical winds is showing that IceLoss_elev gives more physical sound descriptions of the distribution of icing within the wind farm. But there is still one period with a negative slope, 2010-12-01 – 2011-06-30. During the cold part of this period we see in the model data that there are occasions with drier air on higher model levels (used in calculations of ice loads for the turbines at high elevation positions) compared to the lower levels (used in calculations of ice loads for the turbines at low elevation positions). Through sublimation, this will reduce modeled ice load on the higher levels more than on the lower levels. Lower ice loads will lead to lower losses and this explains the negative slope. Factors contributing to the impact on the results are the length of the studied period and the frequency and duration of the icing events in combination with the moisture distribution in the model during the studied period. Low level moisture is a difficult parameter to forecast and further investigations should be made in this area in order to evaluate the performance of the IceLoss_elev model setup.

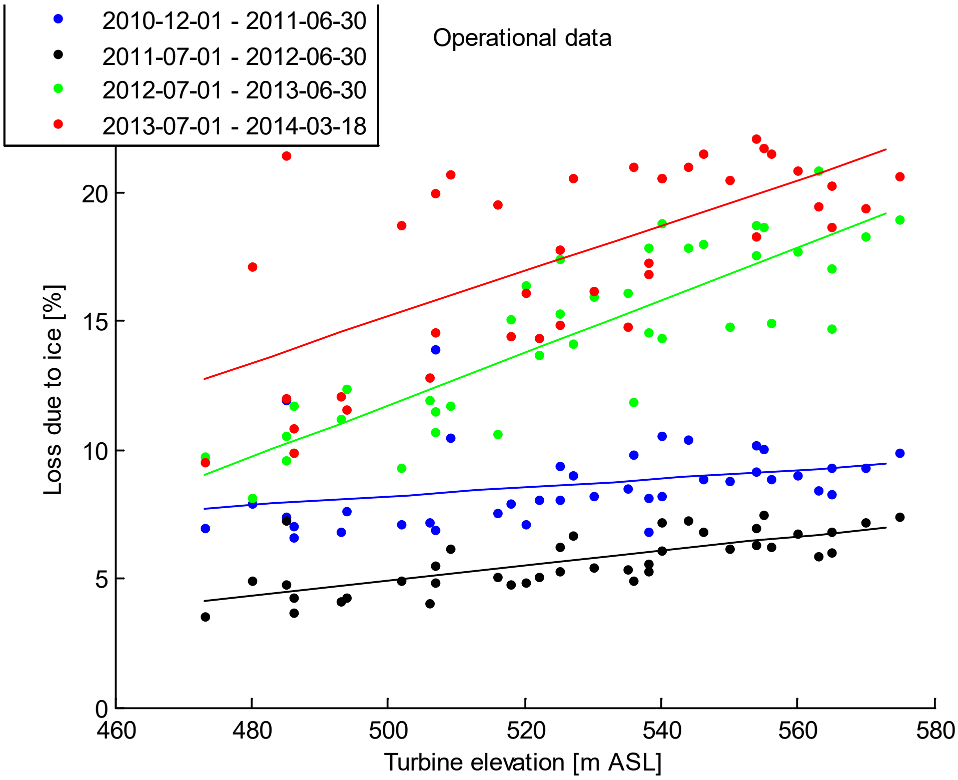

Figure 5-14. The dots represent the yearly loss from individual turbines, based on PEP-PC1. A linear fit to the losses vs. height each year is included to highlight the trends.

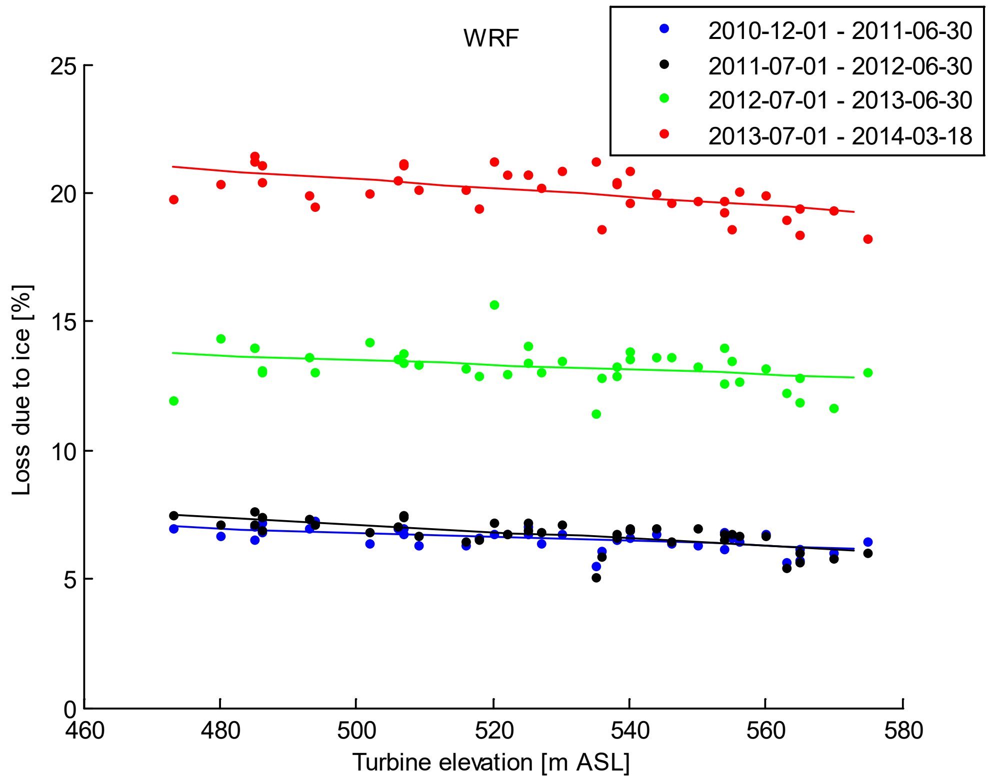

Figure 5-15. The dots represent the yearly loss from individual turbines, based on the IceLoss model run with median power curves and wind transfer coefficients based on operational data. The mean wind farm elevation is used in the calculations. A linear fit to the losses vs. height each year is included to highlight the trends.

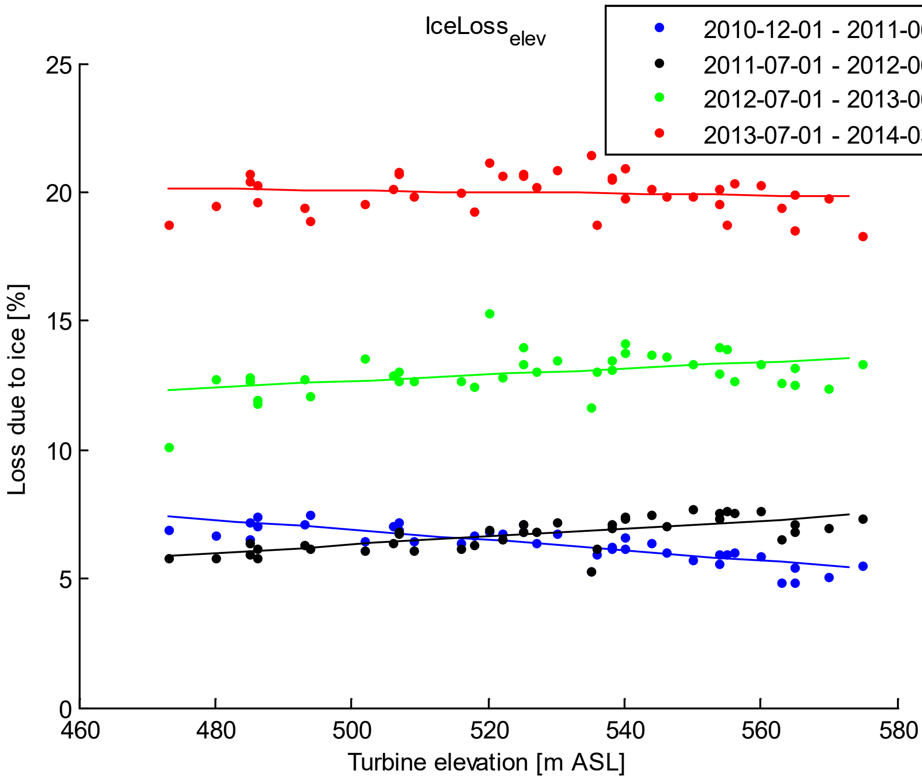

Figure 5-16. The dots represent the yearly loss from individual turbines, based on the IceLoss model run with median power curves and wind transfer coefficients based on operational data. Individual turbine elevation is used in the calculations. A linear fit to the losses vs. height each year is included to highlight the trends.

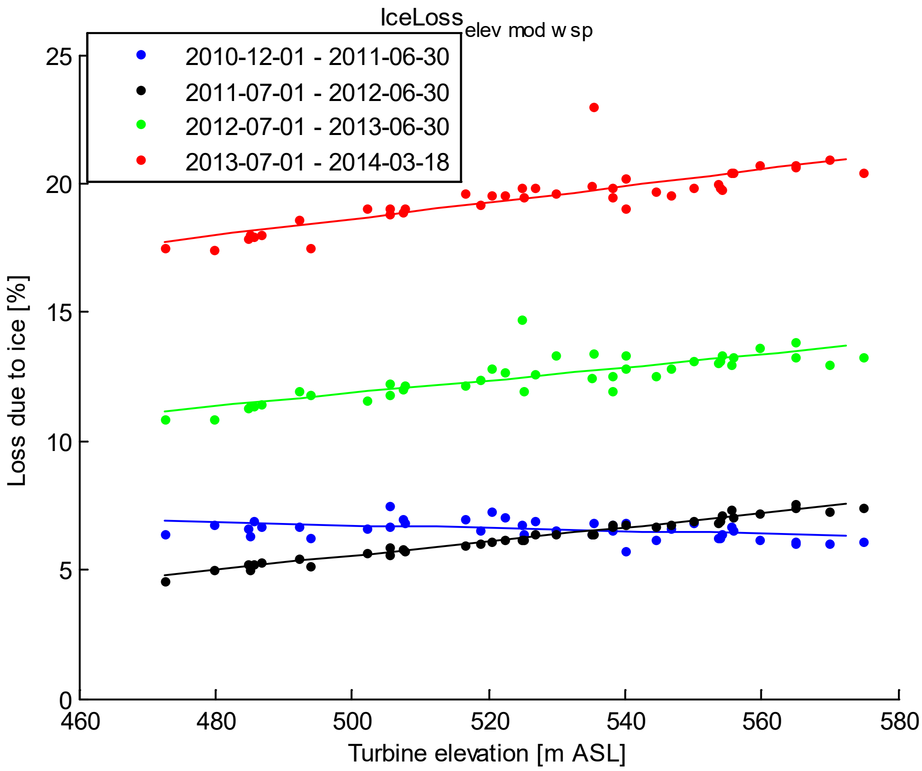

Figure 5-17. The dots represent the yearly loss from individual turbines, based on the IceLoss model run with wind at the turbine locations from the WAsP model. Individual turbine elevation is used in the calculations. A linear fit to the losses vs. height each year is included to highlight the trends.

5.4.1 Investigation of sheltering effects in WF3

Sheltering is when turbines upstream in a wind farm experience more icing than turbines downstream. Several effects are probably involved in the sheltering process.

1. Vertical mixing induced by the rotor

In-cloud icing is creating the most severe icing. When part of the rotor is below the cloud base, it will cause vertical mixing of drier air from below the cloud base into the cloud. This will reduce the super-saturation in the cloud and due to this the efficiency of the icing experienced by the turbines downstream in the wind farm.

2. Ice accretion on the rotor

The super-cooled water droplets are freezing on the turbine blades, reducing the amount of droplets for the turbines downstream.

3. Passage of air across the rotor

The drop in pressure across the rotor, can induce ice particles that is mixed into the wake. The formation of the ice particles will in itself reduce the amount of super-cooled water in the air. But the ice particles will also, via the Bergeron-Findeisen effect, (Bergeron, 1935) grow on the expense of the super-cooled droplets. In addition there will be numerous collisions between the ice particles and the super-cooled droplets in the highly turbulent wake, further reducing the amount of super cooled liquid water in the air.

4. Wind Wake related effects

The reduction of the wind speed in the wakes will make the icing less effective downstream since the ice rate is linearly dependent on the wind speed. An effect that will work in the opposite direction when it comes to losses is the ordinary wind wakes. The relative wake losses will be higher for low wind speeds and this will act to increase the wake losses further downstream in the park.

Now it is investigated if sheltering effects can be seen in WF3.

During the operational period that is used for the analysis, 2010-12-01 – 2014-03-18, icing is found to be most frequent in the 30º wide sectors centered at 30º and 180º. There are distribution differences between the individual winter years, Figure 5-18 , but the two sectors are always among the top when icing is detected and are used to visualize the sheltering effects.

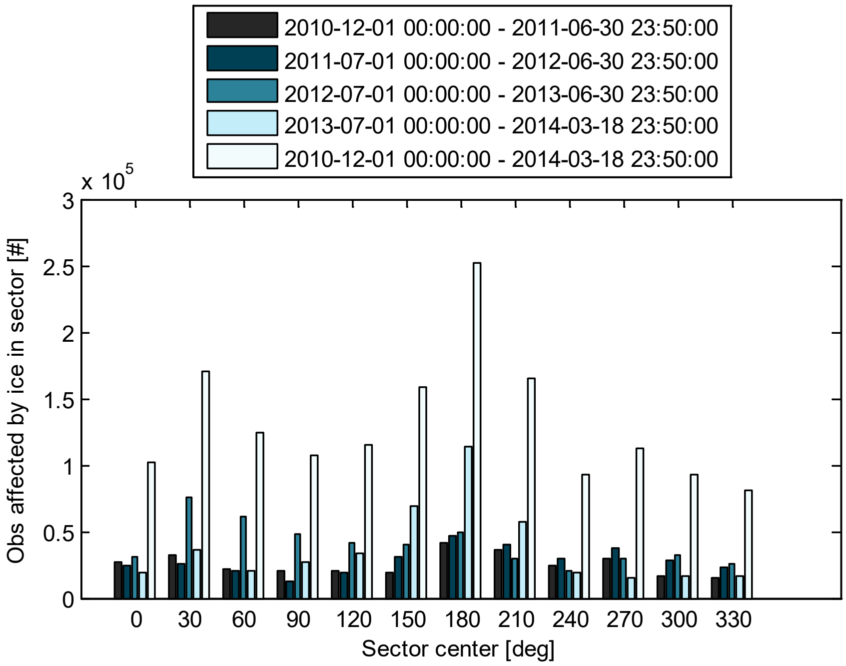

Figure 5-18. Frequency of observations flagged as affected by icing in different sectors for different winter years. The complete period is also included in the figure.

Figure 5-19 is showing the icing loss for the four analyzed winter years with respect to turbine position for the case when the wind is coming from the 30º sector. It is clear that the turbines in the northeast are experiencing more ice than the ones in southwest. There is still a certain degree of height dependence in the icing losses, this can be seen in Figure 5-20 that is showing the icing loss with respect to turbine elevation, but it is not as obvious as when all sectors are considered, Figure 5-14.

The findings for the 180º sector are shown in Figure 5-21 and Figure 5-22. The results from the two sectors show that sheltering effects are present and significant at WF3.

The implications of this is that for wind farms where icing is mainly identified to occur for certain wind directions, certain key turbines could be selected to be retrofitted with de-icing equipment to increase the profitability of the wind farm. For wind farms not yet built, the selection of turbines that should be equipped with de-icing equipment will be based on the icing distribution from a numerical model, adding an extra degree of uncertainty.

One question that this immediately leads to is if the icing is transferred to the downwind turbines when the upwind turbines are equipped with de-icing capabilities? We propose that this question is investigated in a future research project.

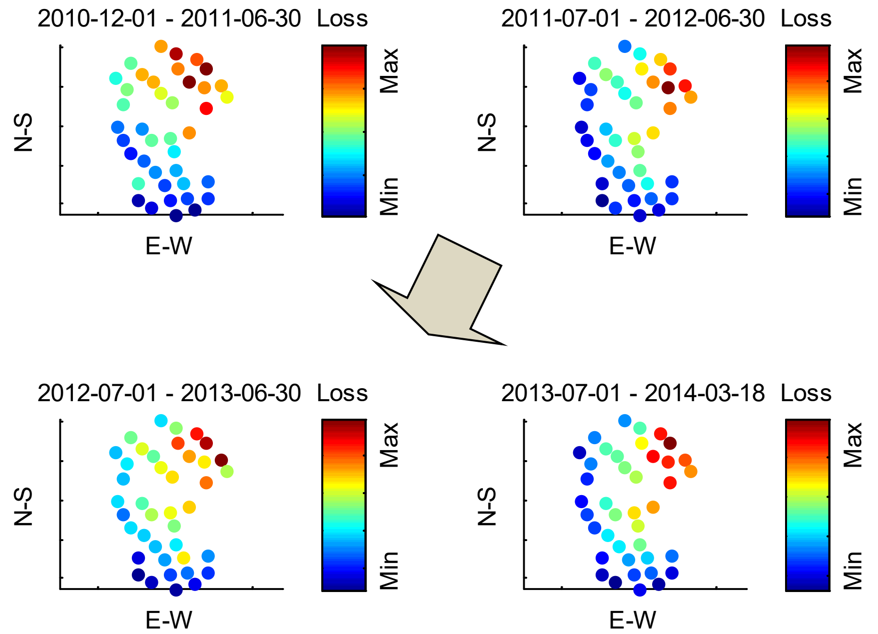

Figure 5-19. The icing loss when the wind is coming from the 30º wide sector, with center at 30º, with respect to turbine position. This is indicated by the arrow in the middle of the figure. Red colors indicate high losses, blue low losses.

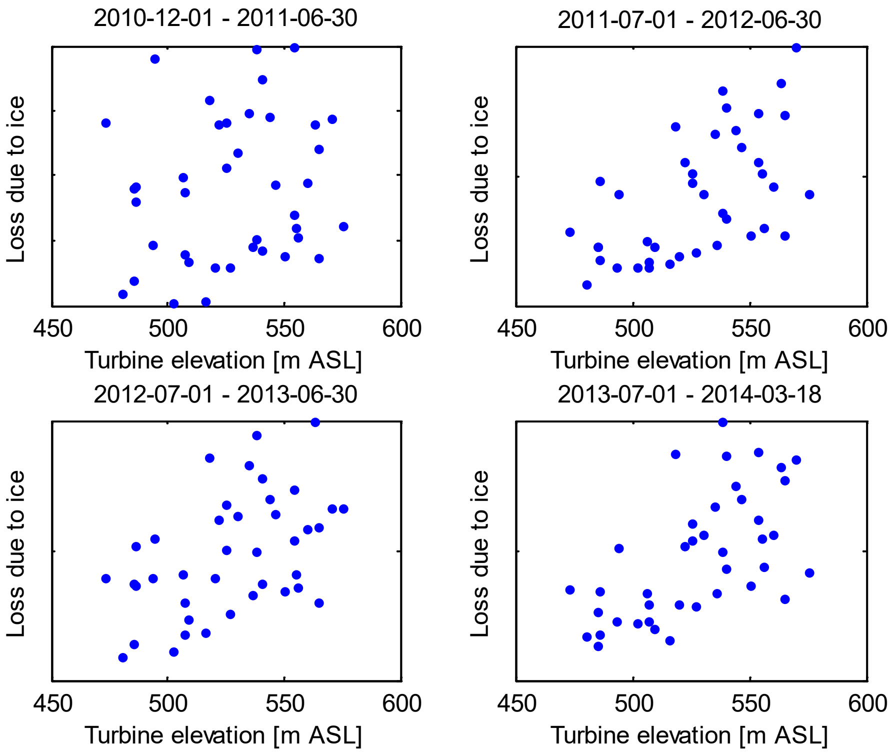

Figure 5-20. The icing loss when the wind is coming from the 30º wide sector, with center at 30º, with respect to turbine elevation.

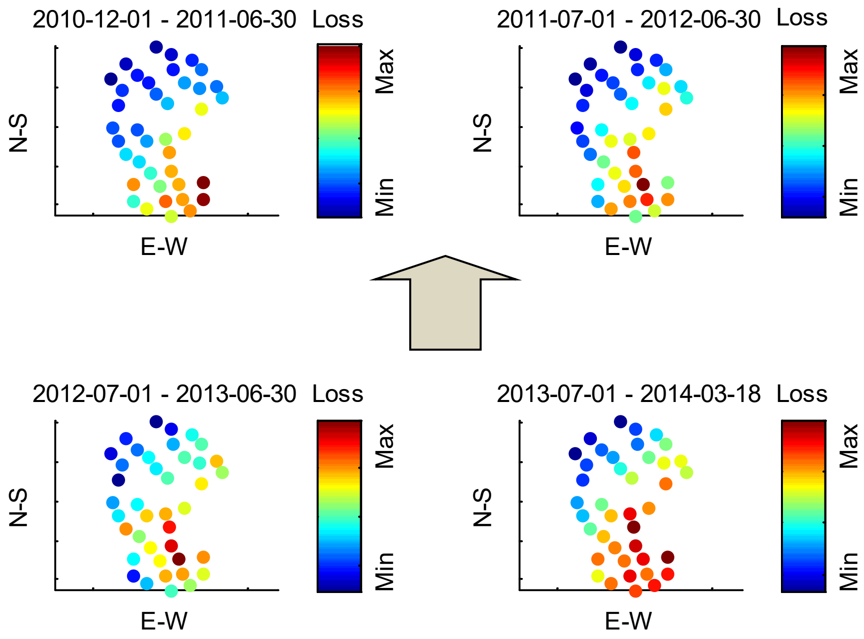

Figure 5-21. The icing loss when the wind is coming from the 30º wide sector, with center at 180º, with respect to turbine position. This is indicated by the arrow in the middle of the figure. Red colors indicate high losses, blue low losses.

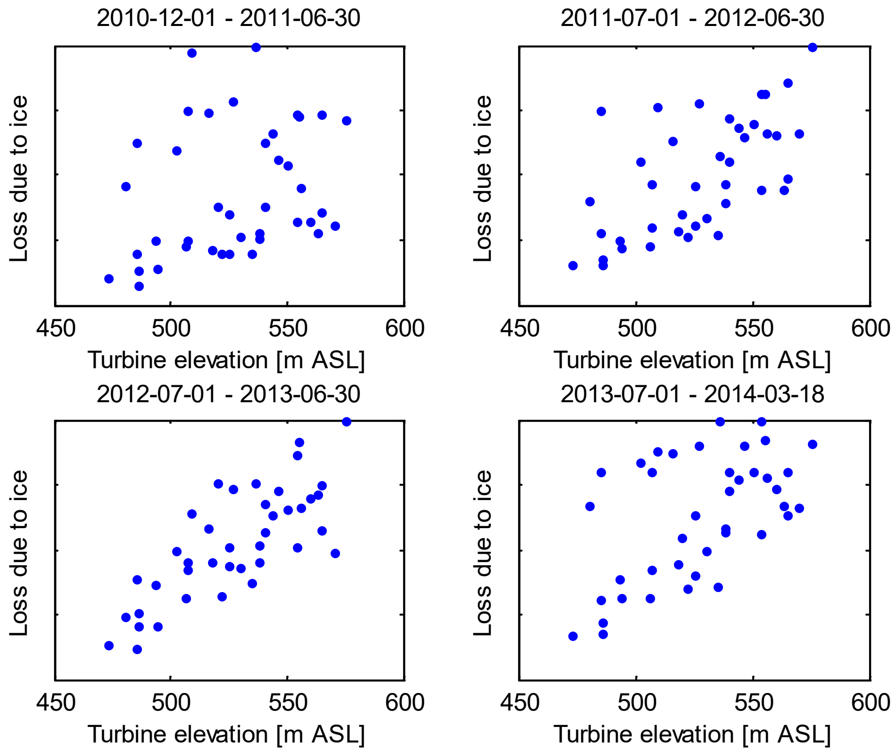

Figure 5-22. The icing loss when the wind is coming from the 30º wide sector, with center at 180º, with respect to turbine elevation.

5.5 CONCLUDING COMMENTS ON CHAPTER 5

In section 5.2 and section 5.4 it is seen that the IceLoss results are agreeing well with the losses estimated from operational data from WF1 and WF3. Hence, we are confident that the model is able to estimate the losses reasonably well. The IceLoss results for WF2 are underestimating the icing losses compared to what is observed. There are indications on that the observed losses might be caused by other ambient conditions than icing. But a deeper investigation of the data points in the direction of icing conditions to be an important factor despite the fact that severe icing conditions are rare in WF2. In the IceLoss calculations it is assumed that the turbines continue to operate with ice on the blades, this assumption is valid for WF1 and WF3, but not for WF2. It is worth noting that the turbines in WF1 and WF3 are from the same manufacturer, while the turbines in WF2 are from another manufacturer.

The IceLoss model has been developed to consider the individual turbine elevation and hub height. Looking at park averages the difference between the original IceLoss and IceLoss_elev are small. This indicates that the assumption used in the original model setup, less icing on turbines on low elevation locations are compensated by more icing on turbines at high elevation locations, is valid and working. Read more in chapter 4 and section 5.2.1.

6 Forecast validation

Daily forecasts during the cold part of the year, October – April, for WF1 and WF3, the wind farms in the project located in areas with rather long winters, are validated. The validation results are presented with respect to forecast lead time. Two different power forecasts are validated

1. No ice is considered (Full)
2. Ice is included in the forecast (Ice)

The forecasts are scaled with transfer coefficients relating the forecast wind speed and the wind speed measured at the nacelle. Median power curves derived from the last winter season are used in combination with the scaled forecast wind speed to calculate the produced energy. In a real-time forecast situation, power curves are based on data before the forecast situation. However, the power curves for all years, according to Table 5.1 and Table 5.3, are similar justifying the approach used in this report.

The park average wind speed and power forecasts are compared with hourly park averages. The park average wind speed and power forecasts are compared with park averages based on observations of nacelle wind speed and power. Data used in the validation are free from alarm or curtailment.

Three validation measures are presented:

1. The mean absolute error (MAE)

$$MAE = \frac{1}{N}\sum_{i=1}^{N}|f_i - y_i|$$

   Where N is the number of forecast /observation-pairs, f_i is the prediction (forecast) and y_i is the true value (measured production).

2. The mean error, or bias (ME)

$$ME = \frac{1}{N}\sum_{i=1}^{N} f_i - y_i$$

   Where N, f_i , y_i have the same meaning as in the mean absolute error.

3. The correlation coefficient (r)

$$r(A,B) = \frac{1}{N-1}\sum_{i=1}^{N}\left(\frac{f_i - \mu_f}{\sigma_f}\right)\left(\frac{y_i - \mu_y}{\sigma_y}\right)$$

Where N is the number of compared value pairs, and μ_f and σ_f are the mean and standard deviation of the forecast f , respectively, and μ_y and σ_y are the mean and standard deviation of the measured production.

6.1 RESULTS WIND FARM 1

Validations are made for the periods November - April 2012-2013, October - April 2013-2014, and October – December 2014.

The results for the wind speed forecasts are seen in Figure 6-1. The results are similar for all three winters. As expected, MEA and ME are increasing with lead time and the correlation is decreasing. Variations between the winters are related to different lengths of validation periods. The fact that the forecast are not constantly being less good with respect to lead time, but vary a bit, is explained by different data availability for different lead times. It is the operational data that is the cause of the difference in data availability.

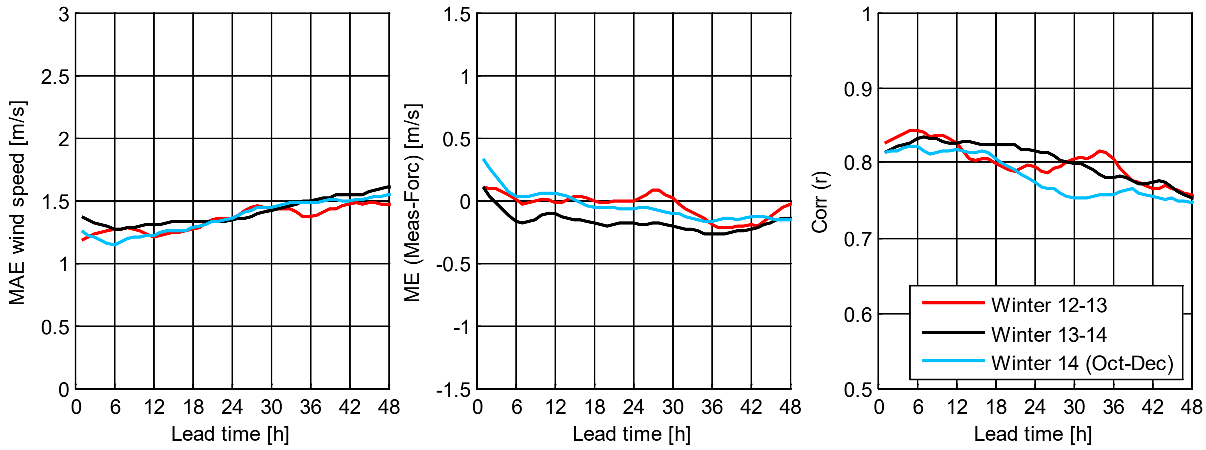

Figure 6-1. Left panel: Mean Absolute Error (MAE). Middle panel: Mean Error (ME), or bias, (measurements – forecast). Right panel: Correlation coefficient. The park average forecasted wind speed is compared with the average of the measured nacelle wind speeds. The result is given with respect to forecast lead time.

The power forecasts are normalized with the total capacity of the wind farm and the same validation measures as for the wind forecasts are presented. There is a significant improvement in the power forecasts when icing is included. The results are found in Figure 6-2, Figure 6-3 and Figure 6-4. The results differ between the winter seasons, this is expected since the amount, and severity, of icing events differ between the years. The last winter is for example based only on the period October – December.

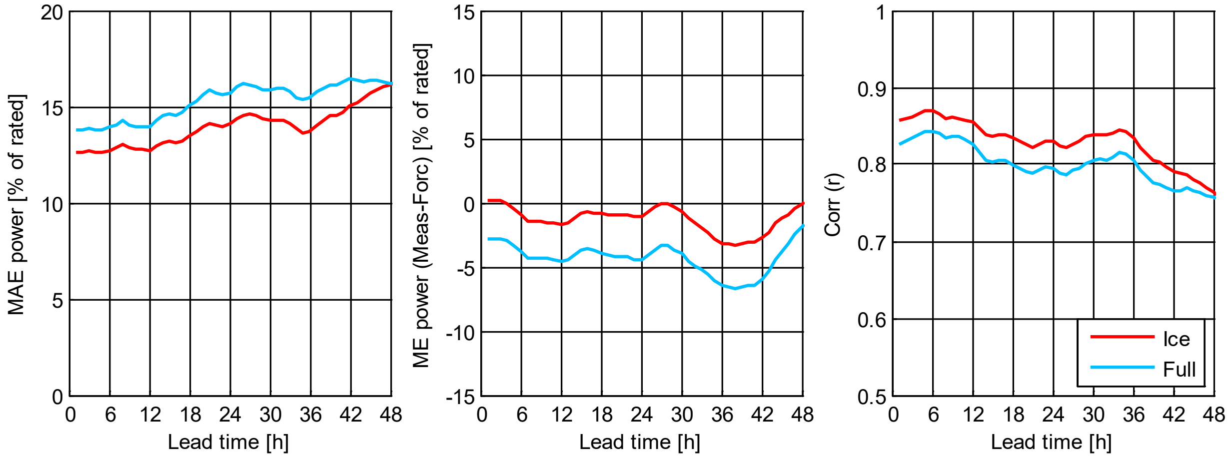

Figure 6-2. Winter 2012-2013. Left panel: Mean Absolute Error (MAE). Middle panel: Mean Error (ME), or bias, (measurements – forecast). Right panel: Correlation coefficient. The park average forecasted power is compared with the park average of the measured power. The blue curve does not include any power reduction due to ice, the red curve includes icing losses.

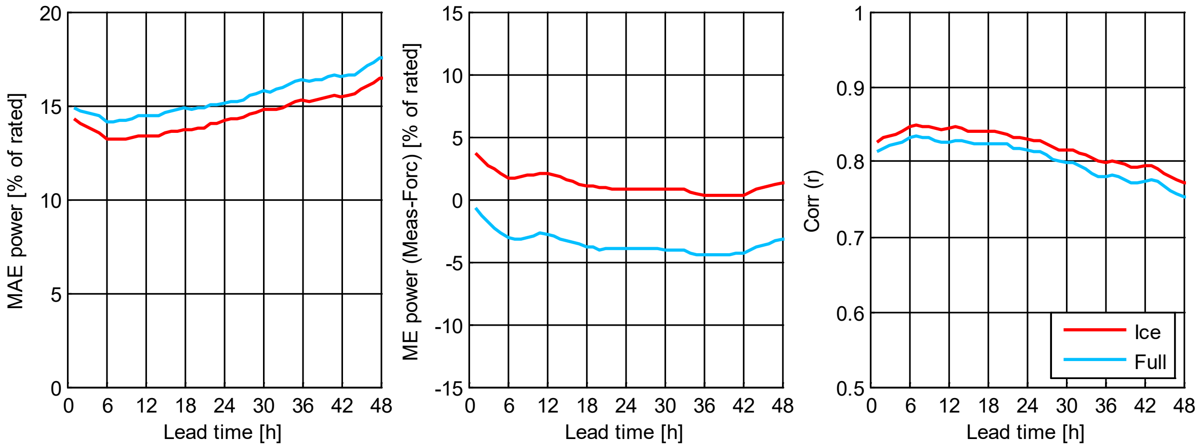

Figure 6-3. As Figure 6-2 but for the winter 2013-2014.

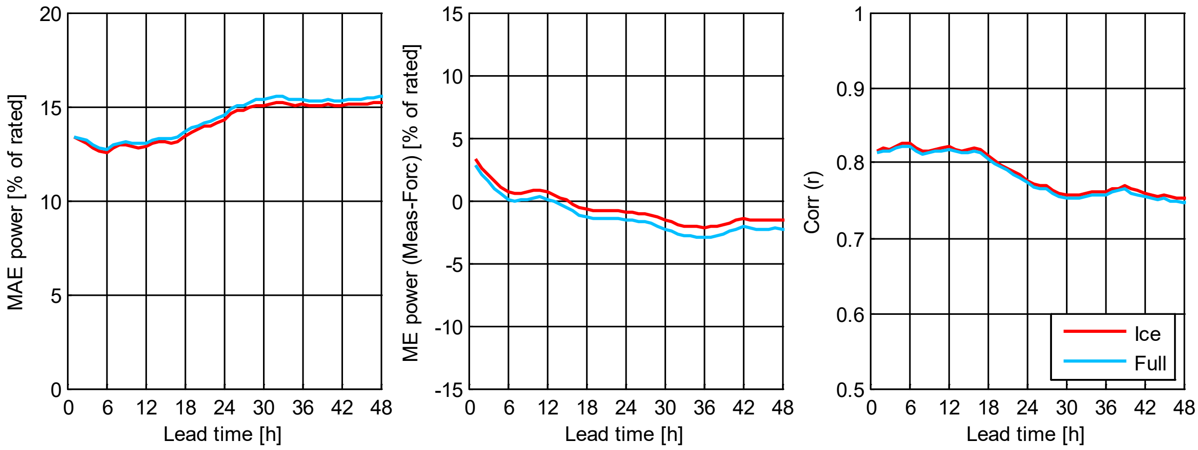

Figure 6-4. As Figure 6-2 but for the period October-December 2014. The difference between the Full and the Ice forecasts is small compared to the other years. Only three months of data is included and the number of icing events was small during the beginning of the winter.

6.2 RESULTS WIND FARM 3

Validations are made for the periods December - April 2012-2013, October - March 2013-2014.

The results for the wind speed forecasts are seen in Figure 6-5. The results are similar for both winters. As expected, MEA and ME are increasing with lead time and the correlation is decreasing. The sudden rise in correlation for longer forecast lead times during the winter 2012-2013 is explained by a high amount of invalid data for those lead times but with a few well performing forecasts left for the comparison. The variations between the winters are related to different lengths of validation periods.

Results for the power forecasts are found in Figure 6-6 and Figure 6-7. Also for WF3 there is a significant improvement in the power forecasts when icing is included. The results for the long lead times in 2012-2013 are affected by the invalid data mentioned above.

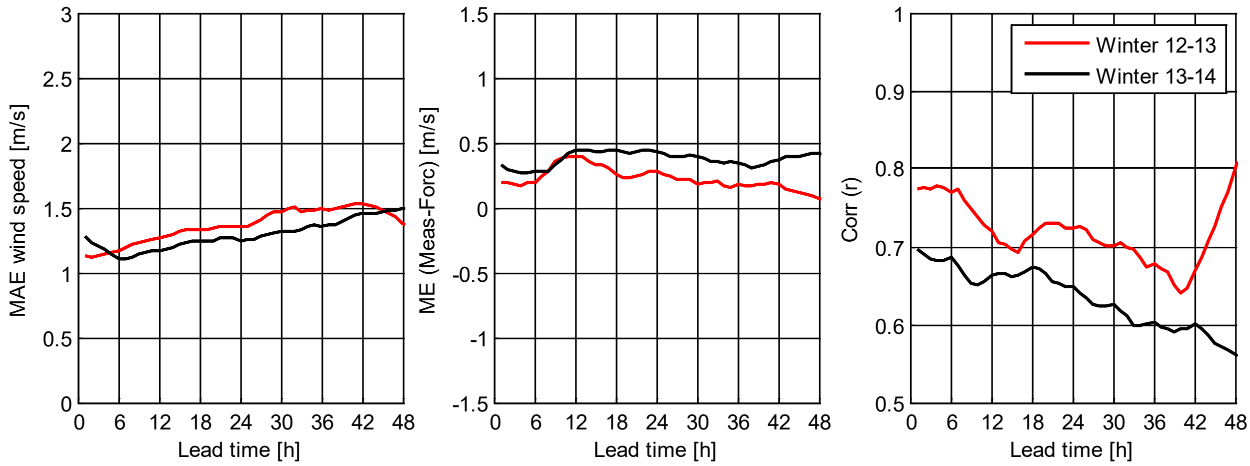

Figure 6-5. Left panel: Mean Absolute Error (MAE). Middle panel: Mean Error (ME), or bias, (measurements – forecast). Right panel: Correlation coefficient. The park average forecasted wind speed is compared with the average of the measured nacelle wind speeds. The result is given with respect to forecast lead time.

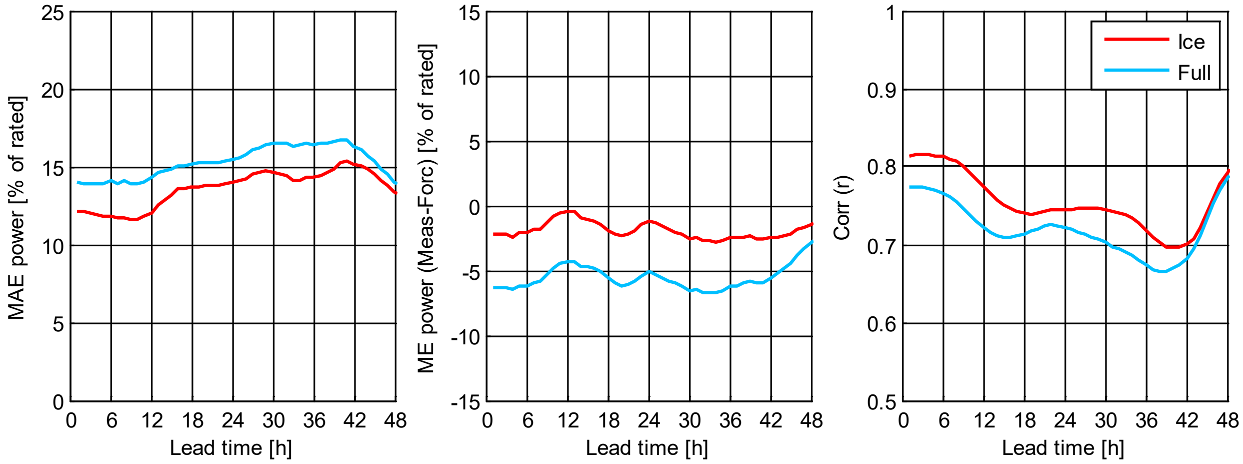

Figure 6-6. December-April 2012-2013. Left panel: Mean Absolute Error (MAE). Middle panel: Mean Error (ME), or bias, (measurements – forecast). Right panel: Correlation coefficient. The park average forecasted power is compared with the park average of the measured power. The blue curve does not include any power reduction due to ice, the red curve includes icing losses.

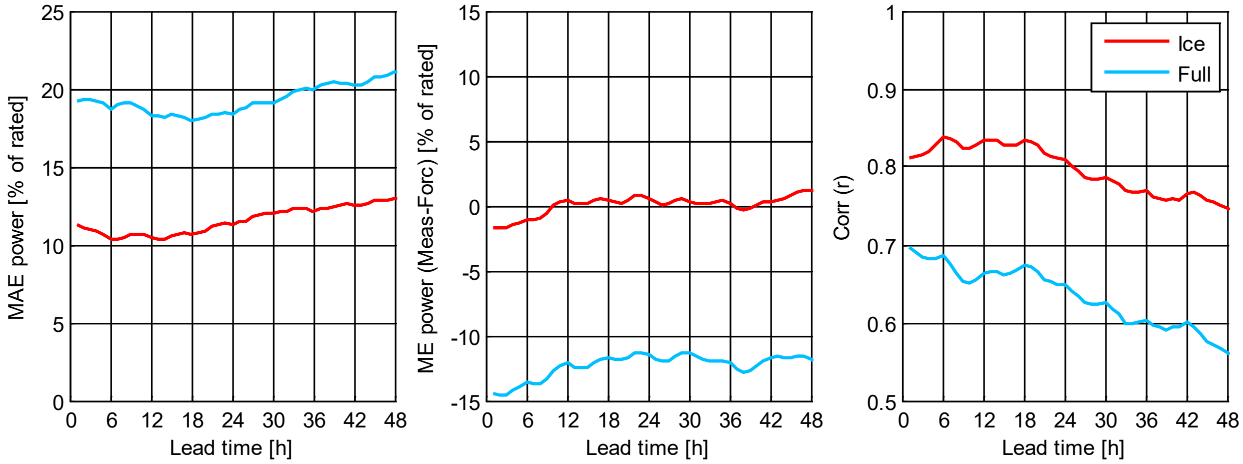

Figure 6-7. As Figure 6-6 but for the period October-March 2013-2014.

7 Nacelle transfer function during icing conditions

Conventional wind turbines have a nacelle mounted anemometer to measure the wind speed. The wind speed is used in the turbine control system. However, the nacelle anemometer is located behind the rotor and is therefore experiencing significant disturbances due to the wind flow around the blades and the nacelle. In order to correct for these effects so that the measured wind speed represents the undisturbed upstream conditions, a correction function called Nacelle Transfer Function (NTF) is applied by the turbine control system to the measured wind speed. Correcting for the wake effects is however a complicated task which is reflected on the accuracy of the NTF. In addition, the NTF might not be valid for the wind flow conditions at the site. Having a nacelle mounted lidar system, in this case a Wind Iris (WI) that measures the wind speed ahead of the rotor gives the possibility of analyzing the nacelle transfer function. In (Turkyilmaz, Hansson, & Undheim, 2016) several evaluations of the NTF are presented.

Here, we investigate possible different characteristics of the NTF (or perhaps more correct, the nacelle anemometer). Note that we don´t have access to the NTF actually used in the turbine control system, instead we derive linear NTFs based on concurrent data from the turbine and the WI. It is also worth noting that the WI itself might disturb the nacelle anemometer and make the NTF that is derived also to be invalid for the site. Therefore an investigation of the possible disturbance of the WI on the nacelle anemometer is made.

Data from a Wind Iris (WI) lidar mounted on turbine 3 in WF1 has been compared with the nacelle anemometer from the same turbine. Information about the measurement campaign and filters applied on the data can be found in (Turkyilmaz, Hansson, & Undheim, 2016). Four measurement campaigns, on four different turbines, have been made in the project, but the one used here is the only one having significant amounts of icing.

Data from the period 2015-01-10 – 2015-04-08 has been used. The WI measurement distance in front of the rotor that is used in the analysis corresponds to 2.2 rotor diameters (D), in this case 200 m. This is consistent with (IEC 61400-12-1, 2005) to avoid blockage effects on the wind flow caused by the rotor.

7.1 POSSIBLE DISTURBANCE OF THE NACELLE ANEMOMETER CAUSED BY WI

The nacelle wind speed measurements from the turbine that the WI is installed on are used as reference. Weekly wind speed ratios between the reference and the neighboring turbines are made for the last two months of the WI measurement campaign and for the two months immediately following the dismantling of the WI. Only periods when the turbines all are experiencing non-wake disturbed wind and are in full performance are used. The installation was made in late December. No ratio comparison is made around the installation. It is difficult to interpret the results when the differences in weekly data availability due to ice filtering are large.

The data coverage and temporal distribution of observations will vary between the weeks. This will induce uncertainties related to different stability conditions, affecting wind shear and wind veer, possibly affecting the nacelle anemometer. But by comparison to the effects of shear and veer on the production, the effect on the anemometer is however expected to be less. At least as long as the turbine can yaw into the wind in a normal way so that the anemometer is not experiencing non-normal wake effects.

Only non-wake sectors are considered in the comparison and it is seen that the distribution of the wind direction observations differ slightly between the two month period before the dismantling and the two month period after the dismantling (Figure 7-1). Note that the scale is different in the two wind roses. It is also seen that there are more high wind observations in the period before the dismantling. These differences will also contribute to the uncertainty.

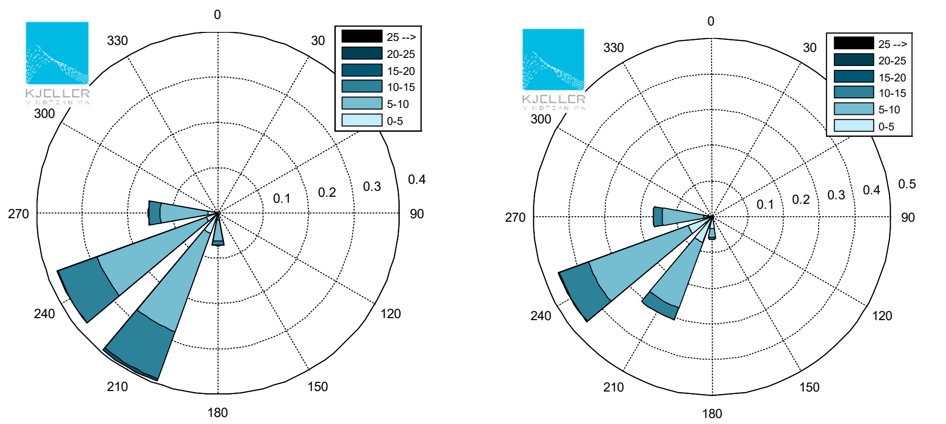

Figure 7-1. Wind speed and direction distribution before (left) and after (right) the installation of the Wind Iris. Note that the scale differs between the two wind roses.

The result, normalized with the maximum value for each turbine, is shown in Figure 7-2. It is worth noting that the maximum values, used for normalization, all are from the period when the WI has been dismantled. The average of all ratios is also found in the figure. The variation in Figure 7-2 is considerable, but it seems like that the nacelle anemometer at the reference turbine is experiencing more wind after the dismantling. This indicates that the WI is influencing the nacelle anemometer. But considering the variability seen in Figure 7-2 it is difficult to put a number on the disturbance. The manufacturer of the WI, Avent, has been asked to comment on the possible disturbance of the nacelle anemometer. According to Avent, previous investigations have not shown substantial influence, provided that the WI is installed according to best practice.

It is important that available recommendations and guidelines are used when a nacelle mounted lidar is installed to minimize the effect of the nacelle anemometer.

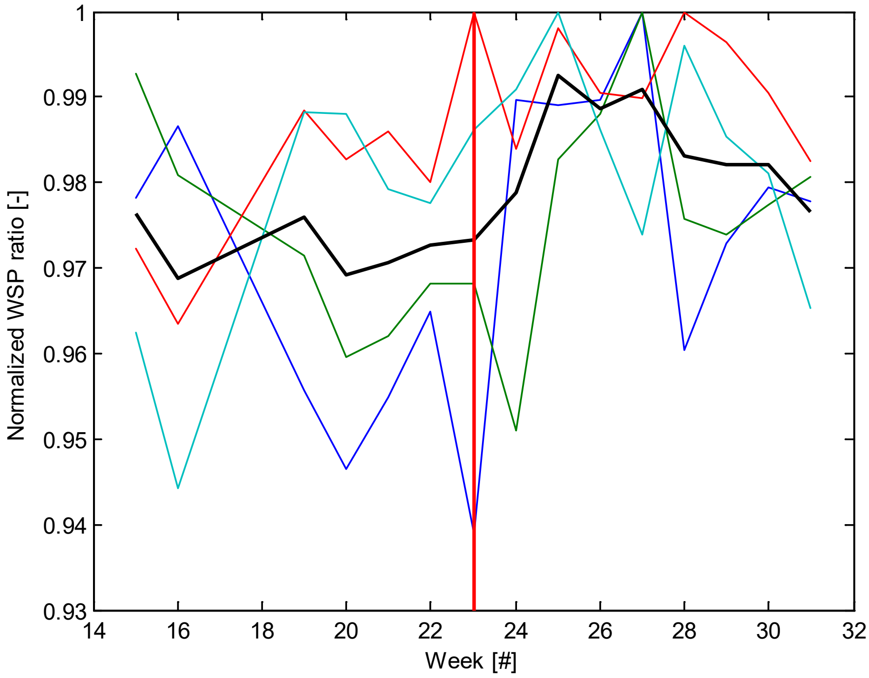

Figure 7-2. The ratio between the wind speed measured by the nacelle anemometer at the turbine where the WI is installed and four neighboring turbines as a function of week number. The ratios are normalized with the maximum values for each series. The black line is the average of all ratios. The red vertical line represents when the WI was dismantled.

7.2 COMPARISON BETWEEN NTF DURING ICING AND NON-ICING CONDITIONS

Figure 7-4 is a scatter plot with WI and nacelle anemometer data during periods when the turbine is in full performance. In the plot is also a linear relationship based on linear regression. The line y = x is included in the plot for reference. A corresponding plot for icing periods is found in Figure 7-5. In an attempt to make the comparison fairer, only wind speeds between 4 m/s and 12 m/s is included in the plots and in the derivation of the linear fits. It is seen that the derived linear relationships deviates from the line y = x. There are several reasons for this. The most obvious is that the NTF is not correct or valid for the site. An invalid NTF can be due to different climatic conditions (turbulence, stability, etc.) compared to where it was derived. The fact that the terrain is not flat will also be of importance. The wind is following the ground and if the turbine position is higher than the ground at the measurement distance, the measured wind will be higher since it is measured higher above the ground. Read more about the effect of the topography in (Turkyilmaz, Hansson, & Undheim, 2016). The occasions with ice during the analyzed period are far less than the occasions without ice. Only the sectors between south and west are included in the comparison. These are the sectors where icing mainly occurs for WF1, Figure 7-3, and using only them will reduce the uncertainty in the comparison due to the effects of different terrain elevations at the measurement range for different directions. However, this will also limit the available data making the results more difficult to interpret. The occasions with ice used in Figure 7-5 seems to cover a wide range of ice loads, Figure 7-7. But as already mentioned, the data set is small and the uncertainty is high.

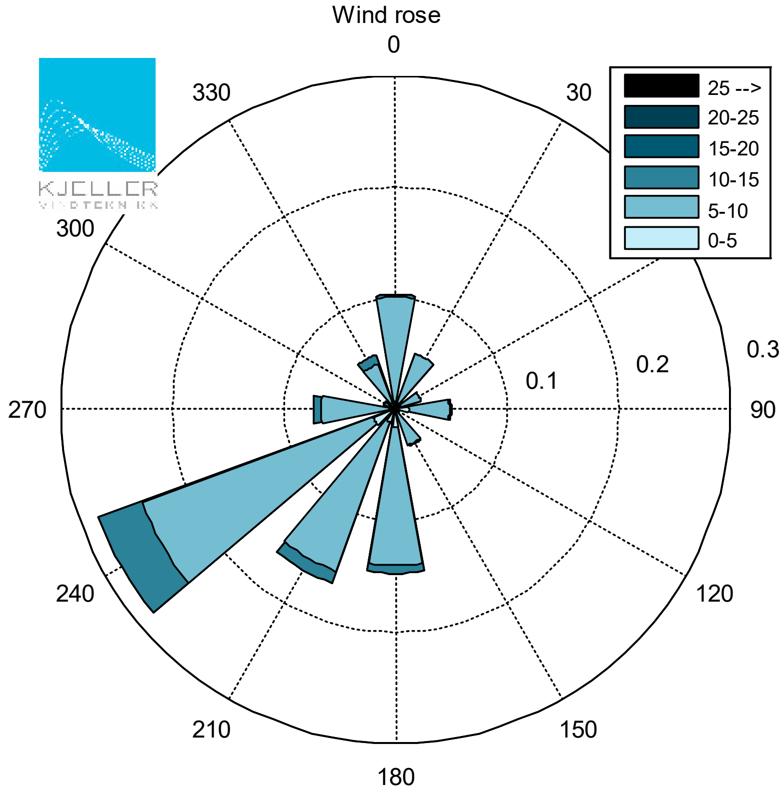

Figure 7-3. Wind rose based on turbine data during occasions with ice on the blades.

The difference between the two linear relationships evaluated for different wind speeds, is found in Figure 7-6. It is seen that the wind speed during icing events is underestimated by the nacelle anemometer for wind speeds up to about 10 m/s. Above 10 m/s it will overestimate the wind speed. This conclusion is based on a small data sample and the uncertainty is considered to be high. And since the results are not clear, the implications of both over and underestimation of the measured wind is discussed below.

1. Given that the results for the interval 4-12 m/s is valid also for higher wind speeds, the true cut-out wind speed during icing events will be lower than expected, possible causing additional losses. The opposite, underestimation of the measured wind speed indicating a true wind speed that is higher than expected, would cause excessive loads on the turbines. Neither effect is desirable.
2. Estimations of production losses during icing events based on the nacelle anemometer (e.g. PEP-PC1) will be dependent on the distribution of wind speed during the investigated period.

WF1 is a low wind speed site and the cut-out problem will most likely be of minor importance. For high wind speed sites this could cause excessive losses (maintenance costs to be higher than expected if the wind is underestimated). The estimation of production losses due to icing is, based on the findings here, problematic when the performance of the wind farm is analyzed. An over(under)estimation of the wind speed will cause the estimation of the full production to be too high(low) if methods (Lindvall, Hansson, & Undheim, 2016) containing the measured wind speed are used. This means that the loss also will be over(under)estimated. The magnitude of the over(under)estimation depends on the distribution of wind speeds on the site.

There are many sources of uncertainty in this comparison

- Different turbine properties during icing and non-icing periods
    - Rotor RPM
    - Pitch angles
- Different wind speed and direction distribution in the two data sets. There will be differences even if we have used only sectors when icing is found to mainly occur.
- Different stability regimes in the two data sets that will affect
    - Turbulence
    - Shear
    - Veer

In a perfect world the findings here should be valid for the particular turbine type in WF1. It is not likely that the results are valid for other turbine types that are operated differently during icing events.

More measurement campaigns during icing periods are needed to study the nacelle anemometer behavior further. Many of the above uncertainties and unknowns can be investigated with multiple, simultaneous, measurements of stability and wind speed from nacelle mounted lidars. This is proposed for future projects.

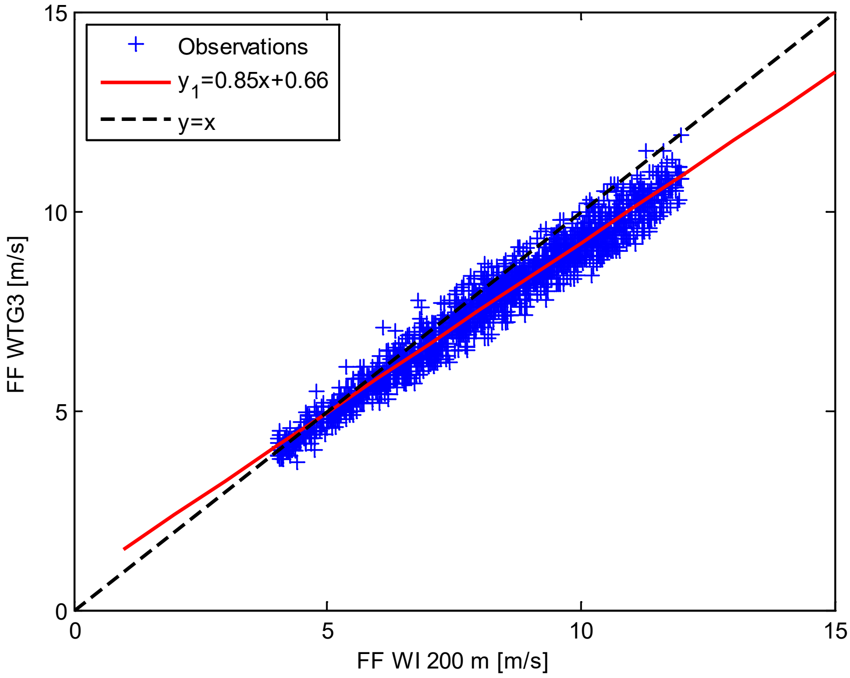

Figure 7-4. The relationship between wind speeds (FF) measured with the nacelle anemometer and wind speeds measured by WI during periods when the turbine is in full performance. All data points marked with blue plus signs are included in the regression used to derive the linear relationship indicated by the red line.

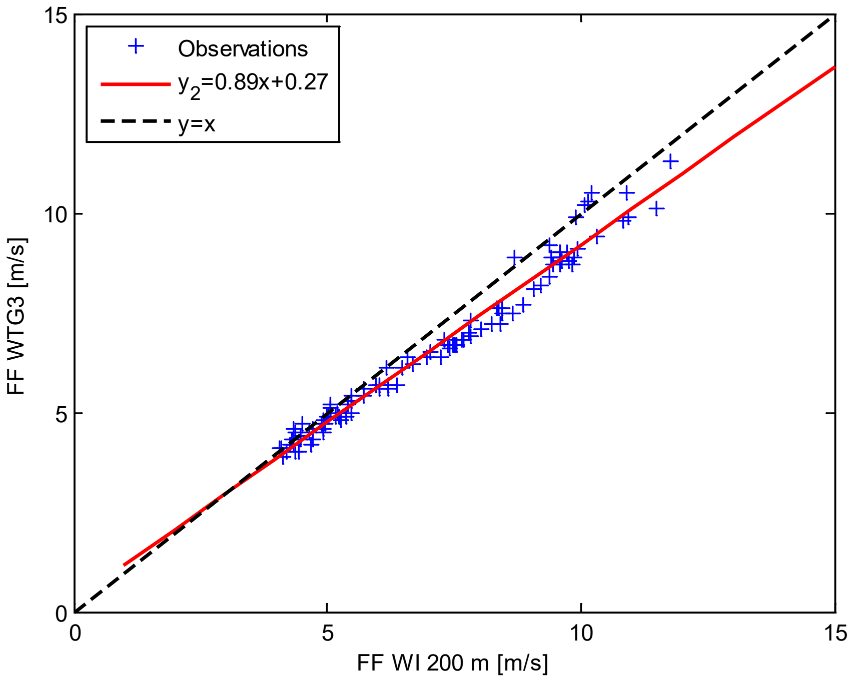

Figure 7-5. The relationship between wind speeds (FF) measured with the nacelle anemometer and wind speeds measured by WI during periods when the turbine is affected by icing. All data points marked with blue plus signs are included in the regression used to derive the linear relationship indicated by the red line.

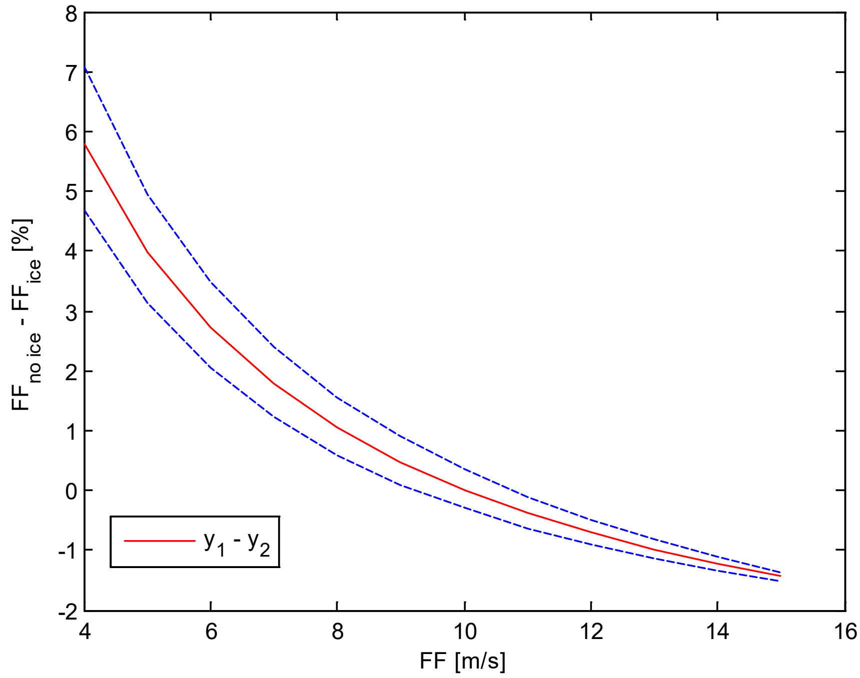

Figure 7-6. The difference between the linear relationships from Figure 7-4 and Figure 7-5 vs. wind speed is shown by the red line. The blue lines indicate an interval that contains at least 50% of the predictions of future predictions at x (wind speed).

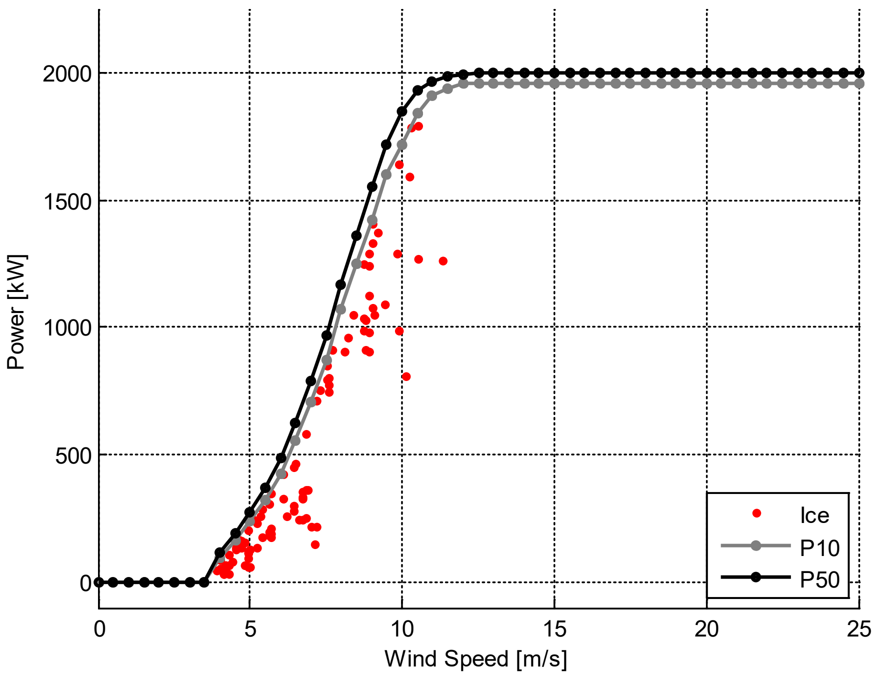

Figure 7-7. Data used in Figure 7-5 is covering a wide range of ice loads (higher ice load corresponds to lower production). The median power curve and the P10-power curve, used for ice detection, is also included in the plot.

8 Conclusions

The main conclusions obtained in the present work are summarized below.

Chapter 3 - Description of methodologies for estimation of icing losses in operational wind farms

- The first challenge is to properly identify when there is ice on the turbine. A threshold power curve in combination with turbine status and a temperature criterion has been used in this report.
- Icing climatologies can be used to estimate long term icing losses. Methods for deriving icing climatologies range between simple assumptions based on publicly available standard meteorological observations, and NWP models in combination with ice accretion models. Icing losses found in operational data can be used to adjust the icing climatology to a site specific value.
- Daily short term forecasts of icing losses are probably exclusively produced by NWP models.

Chapter 4 - Description of the IceLoss model and developments made in this project

- The IceLoss model is originally developed by Kjeller Vindteknikk. It is an advanced model utilizing NWP data to calculate icing rates, ice loads and removal of ice on a standard cylindrical icing collector.
- Losses due to icing on the turbines are calculated by assuming that the turbines continue to operate with ice on the rotor blades where the efficiency is reduced due to the degradation in aerodynamic properties of the blade. It is important to consider the operational strategy of the turbines on sites where they are not allowed to continue to operate with ice on the blades.
- Forecasts are made by tuning the modeled wind speed with transfer coefficients relating nacelle wind speed and model wind speed.
- The IceLoss model makes calculations for the average turbine elevation and the average hub height. In this project, IceLoss is further developed to make calculations for individual turbine elevations and hub heights. It is seen to give a more realistic picture of the icing distribution within the wind farm.
- Short term ice reduced forecasts, valid for the next 48 hours, are produced with IceLoss. The ice reduced forecasts are performing significantly better than the non-reduced forecasts. The initial values of the ice load in the wind farm are taken from the last forecast. In this project, tests have been made in an attempt to use operational data to estimate an initial ice load value for the forecasts. It turned out that it was difficult to estimate the ice load in the wind farm and more research is needed in this area.

Chapter 5 - Post-construction estimation of icing losses

- Median power curves and wind transfer coefficients based on yearly data is used in the estimation of icing losses from the wind farms. It is important to consider revisions in the NTF or turbine control system when deriving the median power curves.

- Sensitivity tests indicate that the IceLoss model calculations made with transfer coefficients and median power curves are robust with respect to erroneous nacelle anemometer measurements. At least as long as the power curves and wind transfer coefficients are based on the same period and from the same data set. In that sense, the improvement of the estimated icing losses based on the IceLoss model used with wind measurements from a nacelle based lidar instead of the nacelle anemometer is limited.

- PEP-PC1 and PEP-PC2 are deemed as suitable for estimating losses due to icing. The other PEP-methods described in (Lindvall, Hansson, & Undheim, 2016) all require at least one turbine to be in full performance to be able to estimate the losses. This is rarely the case during icing occasions.

- The observed icing losses in WF1 and WF3 agree well with estimates from the IceLoss model. The results for WF2 are not as good. The reason is most likely that the turbines are regulated during icing periods in a way that is not part of the assumptions used in the IceLoss model. It is important to consider the operational strategy when losses due to icing are estimated.

- Results from the IceLoss model run with individual turbine elevations are showing a more physical sound distribution of icing in the wind farm when looking at losses for individual turbines. But it is seen in the model data that there are occasions with drier air on higher model levels (used in calculations of ice loads for the turbines at high elevation positions) compared to the lower levels (used in calculations of ice loads for the turbines at low elevation positions). Through sublimation, this will reduce modeled ice load on the higher levels more than on the lower levels. Low level moisture is a difficult parameter to forecast and further investigations should be made in this area in order to evaluate the performance of the IceLoss_elev model setup.

- Sheltering effects (turbines upstream in a wind farm experience more icing than turbines downstream) are significant for some wind directions in WF3. Several effects are probably involved in the sheltering process, vertical mixing induced by the rotor, probably being one of the most important.

- The main contributing factors likely to explain why the modeled production losses in some cases disagree with those estimated from operational data, when considering seasonal time-scales, are noted in the list below. The listed sources of disagreement depend on complex interactions on a wide range of scales that are not very well know at the moment and which are topics of the research community.

    - **Detection of ice in the measured data.** Several methods exist, in this report a 10-percentile threshold power curve is used to detect ice, see Section 5.1. It was the recommended method in (Davis, Byrkjedal, Hahmann, Clausen, & Žagar, 2015) and is used here with minor modifications. The temperature from WRF has been used in the ice detection. The detection would probably be better if high quality temperature measurements from each nacelle were available. The ability to correctly detect occasions with ice on the blades is also depending on the turbine regulation strategy.

  - **Model calculations of ice loads.** There are many different sources of uncertainty in the modelling of ice loads. One of which is the variation in height of the cloud base that can give a large impact on the amount of icing. Another is the partitioning of cloud water into super-cooled droplet and ice crystal when temperatures are below freezing. Other factors contributing to the uncertainties are related to droplet size distributions, initial moisture contents and topographical sheltering effects not resolved by the model.
  - **Model calculations of ice shedding.** The ice load can be very sensitive to melting, sublimation or vibrations that can remove the ice from the blades. This may result in longer or shorter periods of meteorological icing than modelled.
  - **Turbine sensitivity to iced blades.** It is possible that the turbines are more/less sensitive to small amounts of ice than given in the model. The regulation strategies will play an important role here, as seen in WF2 (Chapter 5.3.1). In WF2 it seems like that the turbines sense small amounts of ice and starts a regulation program causing losses.
  - **Characteristics of the nacelle anemometer.** It is assumed that the nacelle anemometer is performing similar during icing and non-icing situations. This is not the case for the measurement campaign analyzed in Chapter 7.

- To better understand how the turbine responds to different ice loads and improve the performance of the IceLoss model, high quality ice load measurements are proposed in future projects.

- The results from WF2 show that the performance of the method for detecting ice on the wind turbines is dependent on turbine regulation strategy. If no details about how the turbine itself is detecting ice are available, ice load measurements could be valuable to improve the knowledge about the regulation strategy. This could in turn be used to improve the ice detection methods by including more SCADA parameters in the filters. The ice load measurements would be used to identify which SCADA parameters that are affected by icing events. This is proposed for future work.

- Our conclusion is that no major improvement in the detection of ice or estimation of losses is expected from using a nacelle mounted lidar.

  - Ice detection is based on a threshold power curve, and a long measurement campaign is necessary to obtain it. Visually, the scatter in the lidar data used to derive the power curve is larger than in the nacelle anemometer data. This indicates that an expensive measurement campaign does not improve the detection of ice on the rotor by this method.

  - It is proposed by VTT in Finland (Karlsson, Peltola, Antikainen, & Vignaroli, 2015) that the risk of ice on the turbine blades could be detected looking at patterns in the backscatter signal from a ground based lidar. This could perhaps also be made with a nacelle based lidar with some modifications in the methodology. However, this project did not have measurements of ice or real-time images needed to investigate the backscatter pattern during verified icing situations.

  - An estimation of losses based on lidar data has the same drawbacks as the ice detection: a long measurement campaign is needed to derive a median power curve for the turbine that the wind speed is applied on. The scatter is also a factor here and the fact that not all sectors will be possible to use due to wakes from other turbines will make it impractical to use.

Chapter 6 - Forecast validation

- When ice is considered in daily production forecasts, the quality is significantly improved.

Chapter 7 - Nacelle transfer function during icing conditions

- The installation of the Wind Iris is made according to best practice (Turkyilmaz, Hansson, & Undheim, 2016). Nevertheless the Wind Iris is found to cause a slight disturbance in the measurements made by the nacelle anemometer.
- Considering that the amount of available data is limited, it is difficult to interpret the comparison between the nacelle anemometer behavior during icing and non-icing conditions. More measurement campaigns are needed.
- There are many sources of uncertainty in this comparison. Among them are
  - Limited amount of icing periods.
  - Only based on one measurement campaign
  - Different turbine properties during icing and non-icing periods
    - Rotor RPM
    - Pitch angles
  - Different wind speed and direction distribution during icing and non-icing periods.
  - Different stability regimes during icing and non-icing periods that potentially affect
    - Turbulence
    - Shear
    - Veer

9 References

Beckford, Lindahl, & Ribeiro. (2015). Quantification and estimation of energy losses caused by blade icing using scada data and pre-construction meteorological masts in the Nordic region.

Bergeron, T. (1935). On the physics of clouds and precipitation. *Proces Verbaux de l'Association de Météorologie, International Union of Geodesy and Geophysics*, pp. 156-178.

Cattin, R. (2012). *Icing of Wind Turbines - Vindforsk projects, a survey of the development and research needs. Elforsk report 12:13.*

Davis, N. N., Byrkjedal, Ø., Hahmann, A. N., Clausen, N.-E., & Žagar, M. (2015). Ice detection on wind turbines using the observed power curve. *Wiley Online Library*.

Harstveit, K. (2009). Using Metar-Data to Calculate in-cloud icing mountain site near by the airport. *Proceedings of IWAIS XIII.* Andermatt, Switzerland.

Hong, S.-Y., Noh, Y., & Dudhia, J. (2006). A new vertical diffusion package with an explicit treatment of entrainment processes. *Monthly Weather Review, 134*, pp. 2318-2341.

IEA. (2012). *IEA Wind Recommended Practice 13: Wind energy in cold climates, Edition 2011.*

IEC 61400-12-1. (2005). *International standard Wind turbines - Part 12-1:Power performance measurments of electricity producing wind tubines. First edition.* IEC.

ISO 12494. (n.d.). *Atmospheric Icing of structures, International Standard, ISO/TC98/SC3/WG6.*

Karlsson, T., Peltola, E., Antikainen, P., & Vignaroli, A. (2015). Lidar as ice detector. *Winterwind.*

Klemp, J. B., Skamarock, W. C., & Dudhia, J. (2000). *Conservative split-explicit time integration methods for the compressible non-hydrostatic equations.* http://www.wrf-model.org.

Lindvall, J., Hansson, J., & Undheim, O. (2016). *Assessment and optimization of the energy production of operational wind farms, Part 1: Post-construction production assessment.* Energiforsk.

Michalakes, J., Dudhia, J., Chen, J., Hart, L., Klemp, J., Middlecoff, J., & Skamarock, W. (2001). "Development of a Next Generation Regional Weather Research and Forecast Model." Developments in Teracomputing: Proceedings of the Ninth ECMWF Workshop on the Use of High Performance Computing in Meteorology. . Singapore: Eds. Walter Zwieflhofer and Norbert Kreitz. World Scientific. 269-27.

Skamarock, W. C., Klemp, J. B., Dudhia, J., Gill, D. O., Barker, D. M., Duda, M. G., . . . Powers, J. G. (2008). *A Description of the Advanced Research WRF Version 3.* Boulder, U.S.: NCAR.

Söderberg, S., & Baltscheffsky, M. (2014). A novel model approach to test de-icing strategies and de-icing efficiency. *Winterwind 2014.* http://www.winterwind.se/sundsvall-2014/presentations-2014/?edmc=2851.

Thompson, Rasmussen, G. R., & Manning, K. (2004). Explicit forecasts of winter precipitation using an improved bulk microphysics scheme. Part 1: Description and sensitivity analysis. *Monthly Weather Review, 117*, pp. 231-235.

Turkia, V., Huttunen, S., & Wallenius, T. (2013). *Method for estimating wind turbine production losses due to icing.* Espoo: VTT.

Turkyilmaz, U., Hansson, J., & Undheim, O. (2016). *Assessment and optimization of the energy production of operational wind farms. Part 2: Use of remote sensing for performance optimization.* Energiforsk.

QUANTIFICATION OF ICING LOSSES IN WIND FARMS

Methods for estimating losses of operational wind farms developed in the Part 1 report are compared with modelled icing losses. It is important to select an appropriate method when icing losses are estimated. Methods based on wind speed, measured or modelled, and measured power is appropriate for periods with icing. It is seen that the operational losses and modelled losses in general are in good agreement.

When icing losses are assessed in operational data and compared to model results, it is important to consider how the turbines are operated during periods with ice on the blades. There can be large discrepancies if the model results are not assuming the actual regulation strategy of the turbine. It is seen in the project that non-optimal regulating strategies can cause unnecessary large losses.

The use of a nacelle mounted lidar is not expected to improve in the detection of ice on the turbine or in the estimation of losses due to icing.

Another step forward in Swedish energy research

Energiforsk – Swedish Energy Research Centre – an industrially owned body dedicated to meeting the common energy challenges faced by industries, authorities and society. Our vision is to be hub of Swedish energy research and our mission is to make the world of energy smarter! We are actively meeting current energy challenges by developing new ways to store energy, helping to create a fossil free transportation system, establishing new market models for the heat and power sector, developing new materials and regulating the grid. www.energiforsk.se

Energiforsk